

# Modelling and simulating Lenski's long-term evolution experiment

Ellen Baake<sup>a,\*</sup>, Adrián González  
Casanova<sup>b</sup>, Sebastian Probst<sup>a</sup>, Anton  
Wakolbinger<sup>c,\*</sup>

<sup>a</sup>University of Bielefeld, Faculty of  
Technology, 33615 Bielefeld, Germany;

<sup>b</sup>Universidad Nacional Autónoma de  
México (UNAM), Instituto de  
Matemáticas, 04510 Ciudad Universitaria,  
México;

<sup>c</sup>Goethe University, Institute of  
Mathematics, 60629 Frankfurt am Main,  
Germany

Email addresses:

ebaake@techfak.uni-bielefeld.de (Ellen  
Baake)

adriangcs@matem.unam.mx (Adrián  
González Casanova)

sprobst@techfak.uni-bielefeld.de (Sebastian  
Probst)

wakolbinger@math.uni-frankfurt.de (Anton  
Wakolbinger)

*Please indicate:* authors in alphabetical  
order.

## \* Corresponding author

Ellen Baake, University of Bielefeld, Fac-  
ulty of Technology, Universitätsstraße 25,  
33615 Bielefeld, Germany, +49-521-106-4896,  
ebaake@techfak.uni-bielefeld.de

**Keywords** — Lenski's long-term evolution  
experiment, epistasis, clonal interference, run-  
time effect, Cannings model, offspring variance

**Declaration of interest:** none

**Role of funding source:** Deutsche  
Forschungsgemeinschaft (German Research  
Foundation, DFG) provided financial support  
via Priority Programme SPP 1590 (Proba-  
bilistic Structures in Evolution, grants no.  
BA 2469/5-2 and WA 967/4-2), but was not  
involved in the study design; in the collection,  
analysis and interpretation of data; in the  
writing of the report; or in the decision to  
submit the article for publication.

## Abstract

We revisit the model by Wiser, Ribeck, and Lenski (Science **342** (2013), 1364–1367), which describes how the mean fitness increases over time due to beneficial mutations in Lenski’s long-term evolution experiment. We develop the model further both conceptually and mathematically. Conceptually, we describe the experiment with the help of a Cannings model with mutation and selection, where the latter includes diminishing returns epistasis. The analysis sheds light on the growth dynamics within every single day and reveals a runtime effect, that is, the shortening of the daily growth period with increasing fitness; and it allows to separate this effect from the contribution of epistasis to the mean fitness curve. Mathematically, we first review the ‘dynamical law of large numbers’ result by González Casanova et al. (Stoch. Proc. Appl. **126** (2016), 2211–2252), which applies in the limit of infinite population size and for an asymptotic parameter regime that excludes clonal interference. We then turn to finite populations and develop approximations and heuristics, among them a refinement and extension of the heuristics by Gerrish and Lenski (Genetica **102/103** (1998), 127–144) for clonal interference. Our findings are supported by simulations for finite populations.

# 1 Introduction

One of the most famous instances in experimental evolution is Lenski’s long-term evolution experiment or LTEE (Lenski et al. 1991; Wiser et al. 2013; Tenaillon et al. 2016; Good et al. 2017). Over a period of 30 years, populations of *Escherichia coli* maintained by daily serial transfer have accumulated mutations, resulting in a steady increase in fitness. The mean fitness is observed to be a concave function of time, that is, fitness increases more slowly as time goes by. Wiser et al. (2013) formulated a theoretical model that builds on the underlying processes, namely mutation, selection, and genetic drift, and obtained a good agreement with the data. However, the model describes the underlying population processes in a heuristic way. As a consequence, one works with effective parameters that are hard to interpret, and it is difficult to disentangle the contributions of the various model components to the resulting fitness curve. González Casanova et al. (2016) recently formulated a microscopic model for a special case (namely, for the case of deterministic fitness increments) and made explicit that the specific design of the LTEE lends itself ideally to a description via a *Cannings model* (Ewens 2004, Ch. 3.3). In a neutral setting, this classical model of population genetics works by assigning in each time step to each of  $N$  (potential) mothers indexed  $j = 1, \dots, N$  a random number  $\nu_j$  of daughters such that the  $\nu_j$  add up to  $N$  and are *exchangeable*, that is, they have a joint distribution that is invariant under permutations of the mother’s indices. In González Casanova et al. (2016), this was extended to include mutation and selection. While Wiser et al. (2013)

work close to the data and perform an approximate analysis in the spirit of theoretical biology, González Casanova et al. (2016) focus on a precise definition of the model and on mathematical rigour (including in particular the proof of a law of large numbers in the infinite population size limit and for a suitable parameter regime).

The goal of this paper is to build a bridge between the two approaches, to generalise the model of González Casanova et al. (2016) to random fitness increments, and to also consider it in the finite-population regime. A thorough mathematical analysis will reveal the many connections between this model and the one of Wiser et al. (2013); in particular, this will make the meaning of its parameters transparent and will allow to separate the effects of the various model ingredients. Parameter identification and stochastic simulations of a suitable extension of the model will make the connection to the experimental data. Let us briefly describe the LTEE and the outline of this paper.

**Lenski’s LTEE.** Every morning, Lenski’s LTEE starts with a sample of  $\approx 5 \cdot 10^6$  *Escherichia coli* bacteria in a defined amount of fresh minimal glucose medium. During the day (possibly after a lag phase), the bacteria divide until the nutrients are used up; this is the case when the population has reached  $\approx 100$  times its original size. The cells then stop dividing and enter a starvation phase. At the end of the growth period, there are therefore  $\approx 5 \cdot 10^8$  bacteria, namely,  $\approx 5 \cdot 10^6$  clones each of average size  $\approx 100$ , see Fig. 1. The next morning, one takes a random sample of  $\approx 5 \cdot 10^6$  out of the  $\approx 5 \cdot 10^8$  cells, puts them into fresh medium,

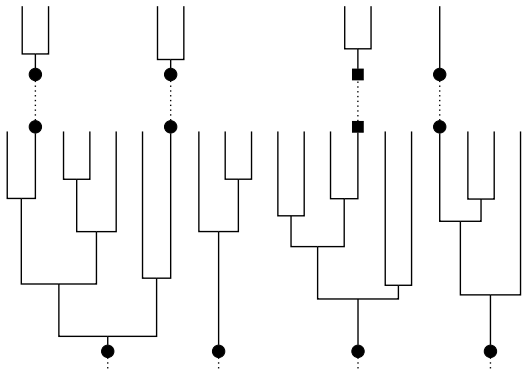


Figure 1: Illustration of some day  $i - 1$  (and the beginning of day  $i$ ) of Lenski's LTEE with 4 founder individuals (bullets), their offspring trees within day  $i - 1$ , and the sampling from day  $i - 1$  to  $i$  (dotted), for an average clone size of 5. The second founder from the left at day  $i - 1$  (and its offspring) is lost due to the sampling, and the second founder from the right at day  $i$  carries a new beneficial mutation (indicated by the square).

and the process is repeated; the sampled individuals are the roots of the new offspring trees. Note that the number of offspring a founder individual contributes to the next day is random; it is 1 on average, but can also be 0 or greater than one.

Lenski started 12 replicates of the experiment in 1988, and since then it has been running without interruption. The goal of the experiment is to observe evolution in real time. Indeed, the bacteria evolve via beneficial mutations, which allow them to adapt to the environment and thus to reproduce faster. Of course neutral and deleterious mutations are more frequent than beneficial ones (Eyre-Walker and Keightley 2007), but neutral

and slightly deleterious mutations will, by definition, contribute nothing or little to the adaptive process, even if they go to fixation; and strongly deleterious ones get lost quickly.

One special feature of the LTEE is that samples are frozen at regular intervals. They can be brought back to life at any time for the purpose of comparison and thus form a living fossil record. In particular, one can, at any day  $i$ , compare the current population with the initial (day 0) population via the following *competition experiment* (Lenski and Travisano 1994; Wiser et al. 2013). A sample from the day-0 population and one from the day- $i$  population, each of the same size, are grown together until the nutrients are used up (say this is the case at time  $T_i$ ). One then defines

$$\begin{aligned} &\text{empirical relative fitness at day } i \\ &= \frac{\log(Y_i(T_i)/Y_i(0))}{\log(Y_0(T_i)/Y_0(0))}, \end{aligned} \quad (1)$$

where, for  $T = 0$  and  $T = T_i$ ,  $Y_i(T)$  and  $Y_0(T)$  are the sizes at time  $T$  of the populations grown from the day- $i$  sample and the day-0 sample, respectively. Note that the empirical relative fitness is a random quantity, whose outcome will vary from replicate to replicate. Fig. 2 shows the time course over 21 years of the empirical relative fitness averaged over the replicate populations, as reported by Wiser et al. (2013). Obviously, the *mean relative fitness* has a tendency to increase, but the increase levels off, which leads to a conspicuous concave shape.

As noted by Wiser et al. (2013), the mean relative fitness may be described by the power law

$$\tilde{f}(k) = (1 + \beta k)^{\frac{1}{2g}} \quad (2)$$

with parameters  $\beta > 0$  and  $g > 0$ . Here  $\beta$  is a time-scaling constant, and the exponent  $g$  de-

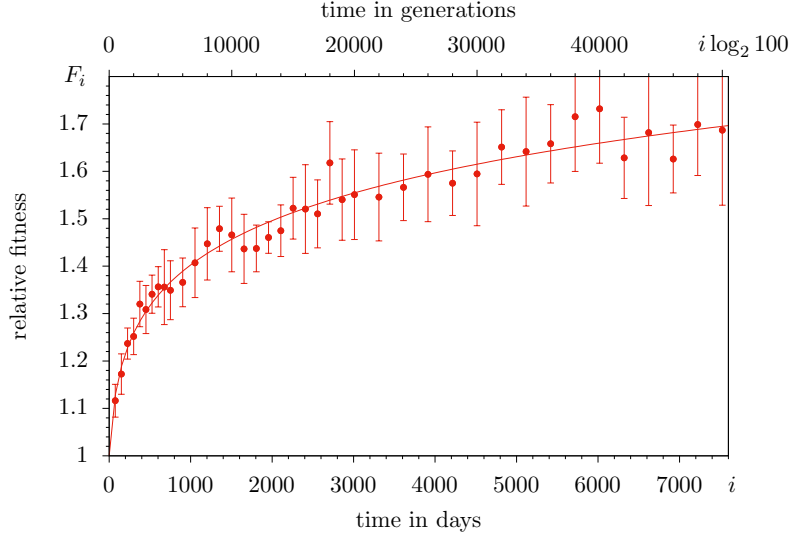


Figure 2: Empirical relative fitness averaged over all 12 populations (red bullets) with error bars (95% confidence limits based on the 12 populations) from Wiser et al. (2013); and corresponding power law (2) with  $\hat{g} = 5.2$  and  $\hat{\beta} = 5.1 \cdot 10^{-3}$  (red solid line). Data and parameters according to Fig. 2A and Table S4 of Wiser et al. (2013).

termines the shape of the curve. Furthermore,  $k$  is time with one generation (which here is the mean doubling time) as unit, so

$$i = \left\lfloor \frac{k}{\log_2 100} \right\rfloor \approx \frac{k}{6.6}. \quad (3)$$

The red solid line in Fig. 2 shows the best fit of this curve to the data of all 12 replicate populations, as obtained by Wiser et al. (2013), with parameter estimates  $\hat{g} = 5.2$  and  $\hat{\beta} = 5.1 \cdot 10^{-3}$ . (Here and in what follows, parameter values estimated from the data are indicated by a hat, and numbers are rounded to 2 digits. Our parameters obtained via `NonlinearModelFit` of `Wolfram Mathematica 11` only differ in the third digits.) In line with (1) and (3), we take *days* as our discrete time units, rather than doubling times (this will pay off in Secs. 2 and

3); so  $\log_2 100 \approx 6.6$  generations in Fig. 2 correspond to one day, and the total of 50000 generations correspond to around 7525 days.

The two models mentioned above aim to explain the power law (2). The one by Wiser et al. (2013), which we will refer to as the WRL model, uses an approach of *diminishing returns epistasis* (which means that the beneficial effect of mutations decreases with increasing fitness (see, e.g., Bürger (2000, p. 74) or Phillips et al. (2000)), Wiser et al. (2013) derive, by partly heuristic methods, a differential equation for the mean relative fitness whose solution is given by (2). The time-scaling parameter  $\beta$  is determined by the interplay of the rate and the effect of beneficial mutations, with the heuristics of Gerrish and Lenski (1998) for the description of clonal interference playing an im-

portant role.<sup>1</sup>

The second approach is the individual-based model of González Casanova et al. (2016) and makes full use of ideas, concepts, and techniques from mathematical population genetics, which seem to be ideally tailored for the LTEE setup. We will address this as the GKWY model; since it has been published in a mathematical journal, we will review it in more detail in Sec. 2 with an emphasis on the biological content. For a certain parameter regime that excludes clonal interference, and using a similar approach to diminishing returns as in the WRL model, González Casanova et al. (2016) prove a law of large numbers as  $N \rightarrow \infty$ , thereby rigorously deriving a version of the power law (2).

**Goal and outline of this paper.** A major goal of this paper is to provide a thorough mathematical model of the LTEE, and to relate it to the observed fitness curve via parameter estimation and stochastic simulations. This approach will provide additional connections between the ideas contained in the WRL and the GKWY models addressed in the previous paragraph. The design of the LTEE, with the daily growth cycles and the sampling scheme, results in an (approximately) constant population size at the beginning of each day. As made explicit by González Casanova et al. (2016), this lends itself in a prominent way to a description

through a Cannings model (including mutation and selection), where the mothers are identified with the founders in a given day and the daughters with the founders in the next day. The crucial parameter of the Cannings model, namely, the *variance of the number of offspring* of a founder individual that make it into the next day, is obtained in the context of the LTEE from an explicit stochastic model of population growth during each day. This offspring variance enters Haldane’s formula for the fixation probability, see (17) below.

As a matter of fact, also Wiser et al. (2013) use a formula for the fixation probability (see Eq. (S1) in their Supplementary Text). In this context they refer to Gerrish and Lenski (1998), who assume a deterministic population growth (and clones of equal size) resulting from synchronous divisions. Indeed, the Cannings model thus hidden within the WRL model turns out to work with a different offspring variance; we will come back to this in Sec. 4.

In addition to the specification of the offspring variance, our model for the daily population growth in continuous time allows us to quantify selection (including diminishing returns epistasis) at the level of the individual reproduction rates within a day. The effect of diminishing returns seems to be obvious from Fig. 2; however, epistasis is not the only contribution to the fitness curve. Rather, the design of the experiment also has its share in it via what we call the *runtime effect*, namely, the shortening of the daily growth phase with increasing fitness. The analysis of our model will allow a clear separation of these contributions. Likewise, the population-genetic notions that also appear in the WRL model (namely, the mutation rate, the selective advantage, the

---

<sup>1</sup>Clonal interference (Gerrish and Lenski 1998; Gerrish 2001; Park and Krug 2007) refers to the situation of two (or more) beneficial mutations present in the population at the same time. They then compete with each other and, in the end, only one of them will be established in the population; an effect that slows down adaption (when measured against the stream of incoming mutations), and biases the distribution of beneficial effects.

effective population size, the fixation probability, and the strength of epistasis) will be made precise in terms of the underlying microscopic model. Throughout, we aim at a rigorous mathematical treatment where possible.

The paper is organised as follows. In Sec. 2, we will recapitulate the GKWY model and explain its law of large numbers (that is a deterministic limit in a suitable parameter regime as population size goes to infinity) for a more biological readership. At the end of Sec. 2, we will consider the resulting stochastic effects in a system whose parameters are obtained from a fit to the data observed in the LTEE (and which thus naturally differs from its infinite population limit). In Sec. 3, this will lead us to consider clonal interference, which is present if the population size is finite in our model. We will investigate clonal interference both for the case of deterministic and random fitness increments. Here we do not prove a law of large numbers, but derive approximations with the help of moment closure and a refined version of the Gerrish-Lenski heuristics. In Sec. 4, we will thoroughly discuss various modelling aspects in the context of both the WRL and the GKWY models, in particular the notions of fitness increment, selective advantage, and epistasis, as well as the equivalent concepts of offspring variance, pair coalescence probability, and effective population size.

## 2 A probabilistic model for the LTEE and its law of large numbers

The GKWY model takes into account two different dynamics, namely, the dynamics *within each individual day*, and the dynamics *from day*

*to day*, together with a suitable *scaling regime*. The resulting *relative fitness process* is proved to converge, in the  $N \rightarrow \infty$  limit, to a power law equivalent to (2); that is, the power law arises as a *law of large numbers*. We explain this here with the help of an appropriate *heuristics*. In what follows, we present these building blocks and perform a first *reality check*.

**Intraday dynamics.** Let  $T$  be (continuous) physical time within a day, with  $T = 0$  corresponding to the beginning of the growth phase (that is, we discount the lag phase). Day  $i$  starts with  $N$  founder individuals ( $N \approx 5 \cdot 10^6$  in the experiment). The reproduction rate (or *Malthusian fitness*) of founder individual  $j$  at day  $i$  is  $R_{ij}$ , where  $i \geq 0$  and  $1 \leq j \leq N$ . It is assumed that at day 0 all individuals have identical rates,  $R_{0j} \equiv R_0$ , so the population is *homogeneous*. Offspring inherit the reproduction rates from their parents.

We use dimensionless variables right away. Therefore we denote by

$$t = R_0 T \quad \text{and} \quad (4)$$

$$r_{ij} = \frac{R_{ij}}{R_0} \quad (5)$$

dimensionless time and rates, so that on the time scale  $t$  there is, on average, one split per time unit at the beginning of the experiment (this unit is 55 minutes, cf. Barrick et al. (2009)) and  $r_{0j} \equiv 1$ . In this paragraph, we consider the  $r_{ij}$  as given (non-random) numbers.

We thus have  $N$  independent *Yule processes* at day  $i$ : all descendants of founder individual  $j$  (the members of the  $j$ -clone) branch at rate  $r_{ij}$ , independently of each other. They do so until  $t = \sigma_i$ , where  $\sigma_i$  is the duration of the growth phase on day  $i$ . We define  $\sigma_i$  as the value of  $t$

that satisfies

$$\begin{aligned} & \mathbb{E}(\text{population size at time } t) \\ &= \sum_{j=1}^N e^{r_{ij}t} = \gamma N, \end{aligned} \quad (6)$$

where  $\gamma$  is, equivalently, the multiplication factor of the population within a day, the average clone size, and the dilution factor from day to day in the experiment ( $\gamma \approx 100$  in the LTEE). Note that the Yule processes are stochastic, so the population size at time  $t$  is, in fact, random; in the definition of  $\sigma_i$ , we have idealised by replacing this random quantity by its expectation. Since  $N$  is very large, this is well justified, because the fluctuations of the random time needed to grow to a factor 100 in size are small relative to its expectation.

**Interday dynamics.** At the beginning of day  $i > 0$ , one samples  $N$  new founder individuals out of the  $\gamma N$  cells from the population at the end of day  $i - 1$ . We assume that one of these new founders carries a *beneficial mutation* with probability  $\mu_N$ ; otherwise (with probability  $1 - \mu_N$ ), there is no beneficial mutation. We think of  $\mu_N$  as the probability that a beneficial mutation occurs in the course of day  $i - 1$  and is sampled for day  $i$ .

Assume that the new beneficial mutation at day  $i$  appears in individual  $m$ , and that the reproduction rate of the corresponding founder individual  $k$  in the morning of day  $i - 1$  has been  $r_{i-1,k}$ . The new mutant's reproduction rate is then assumed to be

$$r_{im} = r_{i-1,k} + \delta(r_{i-1,k}) \text{ with } \delta(r) := \frac{\varphi_N}{r^q}. \quad (7)$$

Here,  $\varphi_N$  is the beneficial effect due to the first mutation (that is  $\delta(1)$ , which applies while

$r = 1$ ), and  $q$  determines the strength of epistasis. In particular,  $q = 0$  implies constant increments (that is, additive fitness), whereas  $q > 0$  means that the increment decreases with  $r$ , that is, we have diminishing returns epistasis. Note that, at this stage, the fitness increment is a *deterministic* function of the mother's reproduction rate. This is in line with the *staircase model* of population genetics (Fisher 1918; Desai and Fisher 2007). We will turn to stochastic increments in Sec 3.2.

Let  $M_i^N$  be the number of new mutants in the sample of size  $N$  at the beginning of day  $i$ . So far we have assumed that  $M_i^N$  can only take the values 1 or 0. More generally, for describing the random number of individuals that are offspring of new mutants from day  $i - 1$  and make it into the  $N$ -sample at the beginning of day  $i$ , we might consider integer-valued random variables  $M_i^N$  with small expectation  $\mu_N$ . We assume that the distribution of  $M_i^N$  does not depend on the current fitness value, and, as in (7), that any mutation adds  $\delta(r) = \varphi_N/r^q$  to the pre-mutant reproduction rate. As long as  $\mu_N$  is not very small, precision may be added by using Poisson random variables, which is what we do in the simulations, see Appendix. One might also think of a finer *intraday modelling* of the mutation mechanism, cf. Wahl and Zhu (2015) or LeClair and Wahl (2018). However, although the limit theorem in González Casanova et al. (2016) is proved only for binary random variables  $M_i^N$ , we conjecture that its assertion also holds for non-binary  $M_i^N$  in the scaling regime (10) discussed below, at least as long as the variances of the  $M_i^N$  remain bounded as  $N \rightarrow \infty$ . We will adhere to the binary assumption in our analysis, and it will turn out as an excellent approximation. Note also that we have idealised by not taking



into account the change in fitness due to mutation during the day; this is because a mutant appearing during the day will not rise to appreciable frequency in the course of this first day of its existence, and thus will not change the overall growth rate of the population in any meaningful way.

**Mean relative fitness.** With a view towards (1) we define the *mean relative fitness*, depending on the configuration of reproduction rates  $r_{ij}$  of the  $N$  individuals in the sample at the beginning of day  $i$ , as

$$F_i^N := \frac{1}{\sigma_i} \log \left( \frac{1}{N} \sum_{j=1}^N e^{r_{ij}\sigma_i} \right). \quad (8)$$

Here,  $\sigma_i$  is as defined in (6). Comparing (1) and (8) we see that the former contains additional sources of randomness: on the one hand, the numerator of (1) may be viewed as stemming from a sample that was drawn from the population at the end of day  $i-1$  (and which consists of individuals different from those present at the beginning of day  $i$ ), on the other hand the duration of the growth phase leading to (1) is not a predicted time as in (8) but an empirical time coming out of the competition experiment between the samples from day  $i$  and day 0. However, since the samples consist of a large number of individuals, the random variables occurring in (1) will, with high probability, come out close to their expectations, thus making already a single copy of the random variable (1) a reasonably good approximation of (8), at least if the population at day  $i$  is sufficiently homogeneous.<sup>2</sup>

---

<sup>2</sup>Indeed, due to the enhanced reproduction rates at day  $i$  compared to day 0, the nutrient consumption time

Note that (8) implies that

$$e^{F_i^N \sigma_i} = \frac{1}{N} \sum_{j=1}^N e^{r_{ij}\sigma_i}. \quad (9)$$

Thus,  $F_i^N$  may be understood as the *effective reproduction rate* of the population at day  $i$ , which is different from the mean Malthusian fitness  $\frac{1}{N} \sum_j r_{ij}$  unless the population is homogeneous, that is,  $r_{ij} \equiv r_i$ .

**Scaling regime.** We have indexed  $\mu_N$  and  $\varphi_N$  with population size because the law of large numbers requires to consider a sequence of processes indexed with  $N$  and to take the limit  $N \rightarrow \infty$ . More precisely, we will take a *weak mutation — moderate selection limit*, which requires that  $\mu_N$  and  $\varphi_N$  become small in some controlled way as  $N$  goes to infinity. Specifically, González Casanova et al. (2016) assume

$$\begin{aligned} \mu_N &\sim \frac{1}{N^a}, \quad \varphi_N \sim \frac{1}{N^b} \text{ as } N \rightarrow \infty, \\ 0 &< b < \frac{1}{2}, \quad a > 3b. \end{aligned} \quad (10)$$

This entails that  $\varphi_N$  is of order greater than  $1/\sqrt{N}$  but of order less than 1. Due to the assumption  $a > 3b$ ,  $\mu_N$  is of much lower order than  $\varphi_N$ . This is used by González Casanova et al. (2016) to prove that, as  $N \rightarrow \infty$ , with high probability no more than two fitness classes are simultaneously present in

---

$T_i$  in the experiment leading to (1) will generically be longer than  $\sigma_i$ , the predicted nutrient consumption time in (8). This is because  $T_i$  refers to a mixture of day- $i$  and day-0 populations (of equal size), whereas  $\sigma_i$  relates to a ‘pure’ day- $i$  population. If the day- $i$  population is homogeneous, this effect will cancel out; but if it is inhomogeneous, (1) will be systematically larger than (8), because then the individuals with a larger reproduction rate will get more weight in (1) than in (8).

the population over a long time span. Note that  $\mu_N$  is the per-day *mutation probability per population* (but see the discussion at the end of the paragraph on interday dynamics).

Furthermore, the scaling of  $\varphi_N$  implies that selection is stronger than genetic drift as soon as the mutant has reached an appreciable frequency. The method of proof applied by González Casanova et al. (2016) requires the assumptions (10) in order to guarantee a coupling between the new mutant's offspring and two nearly critical Galton-Watson processes between which the mutant offspring's size is 'sandwiched' for sufficiently many days. Specifically, under the assumption  $0 < b < \frac{1}{2}$ , the coupling works until the mutant offspring in our Cannings model has reached a small (but strictly positive) proportion of the population, or has disappeared. A careful inspection of the arguments shows that, under the weaker condition  $0 < b < \frac{2}{3}$ , this coupling works at least until the mutant offspring has (either disappeared or) reached size  $N^b$ , from which it then goes to fixation by a law of large numbers argument. This makes the limit result of González Casanova et al. (2016) valid for  $0 < b < \frac{2}{3}$ ; we conjecture that it even holds for  $0 < b < 1$ .

In the case where selection is much stronger than mutation, the classical models of population genetics, such as the Wright-Fisher or Moran model, display a well-known dynamics. Two distinct scenarios can happen, see, e.g., Graur and Li (2000, Ch. 2 and Fig. 2.7): either a fast loss of a new beneficial mutation, or its fixation. We will see that, qualitatively, our Cannings model displays a similar behaviour. Furthermore, as already indicated, with the chosen scaling the population turns out to be homogeneous on generic days  $i$  as  $N \rightarrow \infty$ .

This has the following practical consequences for the *relative fitness process*  $(F_i^N)_{i \geq 0}$  defined by (8). First, on a time scale with a unit of  $1/(\mu_N \varphi_N)$  days,  $(F_i^N)_{i \geq 0}$  turns into a jump process as  $N \rightarrow \infty$ , cf. Fig. 3. Second, on the (generic) days  $i$  at which the populations are nearly homogeneous, the subtle systematic difference between (1) and (8), as described in Footnote 2, will disappear.

**Heuristics leading to the limit law.** Assume a new mutation arrives in a *homogeneous* population of relative fitness  $F$ . It conveys to the mutant individual a relative *fitness increment*

$$\delta_N(F) = \frac{\varphi_N}{F^q}, \quad (11)$$

that is, the mutant has relative Malthusian fitness  $F + \delta_N(F)$ . The length of the growth period then is

$$\sigma(F) = \frac{\log \gamma}{F} \quad (12)$$

(since this solves  $e^{Ft} = \gamma$ , cf. (6)). We now define the *selective advantage* of the mutant as

$$s_N(F) = \delta_N(F) \sigma(F). \quad (13)$$

Obviously, *the length  $\sigma$  of the growth period decreases with increasing  $F$*  and, since  $s_N$  in (13) decreases with decreasing  $\sigma$ ,  $s_N$  would decrease with increasing  $F$  even if  $\delta_N(F)$  were constant. This is what we call the *runtime effect*: adding a constant to an interest rate  $F$  of a savings account becomes less efficient when the runtime decreases.

Let us explain the reasoning behind (13). In population genetics, the selective advantage (of a mutant over a wildtype) per generation is

$$s = \frac{a_1 - a_0}{a_0}, \quad (14)$$

where  $a_0$  ( $a_1$ ) is the expected number of descendants of a wildtype (mutant) individual in one generation; Eq. (14) has the form of a *return* (of a savings account, say). If growth is in continuous time with Malthusian parameters  $r_0$  and  $r_1 = r_0 + \delta$ , respectively, and a generation takes time  $\sigma$ , then  $a_0 = e^{r_0\sigma}$  and  $a_1 = e^{r_1\sigma} \approx a_0(1 + \delta\sigma)$  if  $\delta$  is small, which turns (14) into (13). Often, the appropriate notion of a generation is the time until the population has doubled in size, see e.g. Eq. (3.2) in Chevin (2011), which provides an analogue to (13). In our setting, the corresponding quantity is the time required for the population to grow to  $\gamma$  times its original size, which is the length  $\sigma(F)$  of the growth period in (12).<sup>3</sup> Together with the above expression for  $s$ , this explains (13). Notably, a formula that is perfectly analogous to (13) also appears in Sanjuán (2010, p. 1977, last line); there, the concept of a viral generation is associated with the cell infection cycle, and the number  $K$  (which corresponds to our  $\gamma$ ) is the burst size or viral yield per cell.

Furthermore, it is precisely this notion of selection advantage conveyed by (13) and (14) that governs the *fixation probability*. Namely, the fixation probability of the mutant turns out to be

$$\pi_N(F) \sim C s_N(F). \quad (15)$$

Here,  $\sim$  means asymptotic equality<sup>4</sup>, and  $C := \gamma/(\gamma - 1)$  is asymptotically twice the reciprocal offspring variance in one Cannings generation of the GKWY model<sup>5</sup>; that is, with the nota-

tion introduced in the first paragraph of the Introduction, the offspring variance  $v$  in one Cannings generation satisfies

$$v = \mathbb{V}(\nu_1) \sim 2 \frac{\gamma - 1}{\gamma} = \frac{2}{C}. \quad (16)$$

Hence (15) is in line with Haldane's formula

$$\pi \sim \frac{s}{v/2}, \quad (17)$$

which says that the fixation probability  $\pi$  is (asymptotically) the selective advantage  $s$  divided by half the offspring variance  $v$  in one generation. Haldane's formula relies on a branching process approximation of the initial phase of the mutant growth; see Patwa and Wahl (2008) for an account of this method, including a historic overview.

For the sake of completeness, let us give the following intuitive explanation for (16). In every Cannings model, one has the relation

$$v = (N - 1)p_{\text{coal}} \quad (18)$$

between  $v$  and the pair coalescence probability  $p_{\text{coal}}$ , that is, the probability that two randomly sampled daughters have the same mother, cf. Durrett (2008, Ch. 4.1). Eq. (18) then follows readily from the elementary relation  $p_{\text{coal}} = \mathbb{E}[\frac{1}{N(N-1)} \sum_j \nu_j(\nu_j - 1)]$ , which, in turn, equals  $\frac{1}{N-1}(\mathbb{E}[\nu_1^2] - 1) = \frac{1}{N-1}v$ , because the  $\nu_j$  are exchangeable and sum to  $N$  by assumption. In our specific Cannings model, the family size of a randomly sampled daughter individual at the end of the day is, on average, asymptotically twice as large as a typical family size<sup>6</sup>. Since we have  $N$  clones of average size

<sup>3</sup>In line with this, we choose days as our discrete time units, as already mentioned in Sec. 1.

<sup>4</sup>That is,  $\pi_N(F)/(C s_N(F)) \rightarrow 1$  as  $N \rightarrow \infty$ , see González Casanova et al. (2016).

<sup>5</sup>Let us emphasise once again that one generation of this Cannings model corresponds to one day in the LTEE.

<sup>6</sup>The size of the clone to which a sampled individual belongs has a *size-biased* distribution; this is in line with

$\gamma$ , and the sampling is without replacement, we have

$$p_{\text{coal}} \sim \frac{2}{N} \frac{\gamma - 1}{\gamma}. \quad (19)$$

Together with (18) this implies (16). Note that (19) at the same time defines the (coalescence) effective population size via  $N_e = 1/p_{\text{coal}}$ , cf. Ewens (2004, Ch. 3.7) or Durrett (2008, Ch. 4.4).

Another crucial ingredient of the heuristics is the time window of length

$$u_N(F) = \frac{\log N}{s_N(F)} \quad (20)$$

after the appearance of a beneficial mutation that will survive drift (a so-called *contending mutation*) in the fitness background  $F$ ; this approximates the expected time it takes for the mutation to become dominant in the population. Indeed, (20) is asymptotically equivalent to the solution of

$$(1 + s_N)^i = \varepsilon N$$

for any positive constant  $\varepsilon$ ; here, the left-hand side is the expected offspring size of a mutant

---

the classical *waiting time paradox* (cf. Georgii (2013, Example 4.16)). In our model, the size distribution of a typical clone at the end of the day is approximately geometric with parameter  $1/\gamma$ , and the size-biasing of this distribution is (approximately) negative binomial with parameters 2 and  $1/\gamma$ . Consequently, the expected size of the clone to which a sampled individual belongs is approximately  $2\gamma$ , that is twice the expected size of a typical clone. This proportion carries over from the clones to the families of sampled individuals. Let us emphasise once again that a *family* consists of the founders at the beginning of the next day that go back to the same founder in the current day; whereas a *clone* consists of all descendants of a founder at the end of a day, regardless of whether they are sampled for the next day or not.

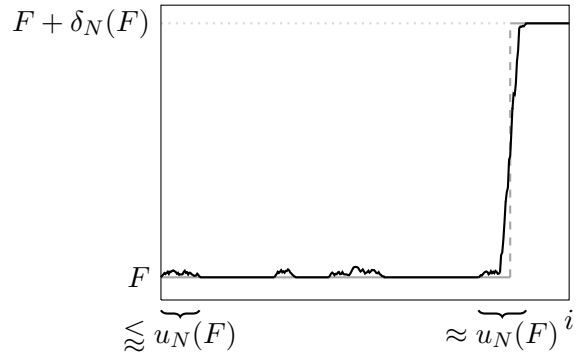


Figure 3: The relative fitness process (black) and the approximating jump process (grey).

after  $i$  days in the branching process approximation, and the right-hand side is a sizeable proportion of the population.

All this now leads us to the dynamics of the relative fitness process. As illustrated in Fig. 3, most mutants only grow to small frequencies and are then lost again (due to the sampling step). But if it does happen that a mutation survives the initial fluctuations and gains appreciable frequency, then the dynamics turns into an asymptotically deterministic one and takes the mutation to fixation quickly, cf. Durrett (2008, Ch. 6.1.3). Indeed, within time  $u_N(F)$ , the mutation has either disappeared or gone close to fixation; by (10), this time is much shorter than the mean interarrival time  $1/\mu_N$  between successive beneficial mutations. As a consequence, there are, with high probability, at most two types present in the population at any given time (namely, the *resident* and the *mutant*), and *clonal interference is absent*. Therefore, in the scenario considered, survival of drift is equivalent to fixation.

Next, we consider the expected per-day increase in relative fitness, given the current value

$F$ . This is

$$\begin{aligned}\mathbb{E}(\Delta_N F | F) &\approx \mu_N \pi_N(F) \delta_N(F) \\ &\sim \frac{\Gamma_N}{F^{2q+1}}.\end{aligned}\quad (21)$$

Here, the asymptotic equality is due to (11)–(13) and (15), and the compound parameter

$$\Gamma_N := C\mu_N\varphi_N^2 \log \gamma \quad (22)$$

is the rate of fitness increase per day at day 0 (where  $r_{0j} \equiv F_0 = 1$ ). Note that  $\varphi_N/F^q$  appears squared in the asymptotic equality in (21) since it enters both  $\pi_N$  and  $\delta_N$ . Note also that the additional +1 in the exponent of  $F$  comes from the factor of  $1/F$  in the length of the growth period (12), and thus reflects the runtime effect.

This now leads us to define a new time variable  $\tau$  related to  $i$  of (3) via

$$i = \left\lfloor \frac{\tau}{\Gamma_N} \right\rfloor \quad (23)$$

with  $\Gamma_N$  of (22), which means that one unit of time  $\tau$  corresponds to  $\Gamma_N$  days. With this rescaling, we have

$$F_{\lfloor \tau/\Gamma_N \rfloor}^N \rightarrow f(\tau) \text{ as } N \rightarrow \infty,$$

where  $f$  satisfies the initial value problem

$$\frac{d}{d\tau} f(\tau) = \frac{1}{f^{2q+1}(\tau)}, \quad f(0) = 1, \quad (24)$$

with solution

$$f(\tau) = (1 + 2(1 + q)\tau)^{\frac{1}{2(1+q)}}. \quad (25)$$

Note that (24) is just a rescaling limit of (21), where the expectation was omitted due to the scaling regime applied, as will be explained next.

**Law of large numbers.** The precise formulation of the limit law (González Casanova et al. 2016) reads

**Theorem** *For  $N \rightarrow \infty$  and under the scaling (10), the sequence of processes  $(F_{\lfloor \tau/\Gamma_N \rfloor}^N)_{\tau \geq 0}$  converges, in distribution and locally uniformly, to the deterministic function  $(f(\tau))_{\tau \geq 0}$  in (25).*

The theorem was proved along the heuristics outlined above<sup>7</sup> with the help of advanced tools from probability theory. It is a law of large numbers reasoning, which allows to go from (21) to (24) (and thus to ‘sweep the expectation under the carpet’), in the sense that, for large  $N$  and under the scaling assumption (10), fitness is the sum of a large number of small per-day increments accumulated over many days, and may be approximated by its expectation.

Since time has been rescaled via (23), Eq. (25) has  $q$  as its single parameter. Note that  $1/(2(1+q)) < 1$  (leading to a concave  $f$ ) whenever  $q \geq 0$ ; in particular, *the fitness curve is concave even for  $q = 0$ , that is, in the absence of epistasis*. This is due to the runtime effect: if the population as a whole already reproduces rather fast, then the end of the growth phase is reached sooner and thus leaves less time for a mutant to play out its advantage; see also the discussion in Sec. 4. The second parameter, namely  $\Gamma_N$ , reappears when  $\tau$  is translated back into days; that is,  $F_i^N \approx f(\Gamma_N i)$ . Note that  $R_0$ , as used in the first nondimensionalisation step (4), is not an additional parameter because it is already absorbed in  $\varphi_N^2$ .

**A first reality check.** The limit law (25) is identical with the power law (2) of Wiser et al.

<sup>7</sup>Note that González Casanova et al. (2016) partly work with dimensioned variables, which is why the notation and the result look somewhat different.

(2013) up to a transformation of the parameters that relies on relevant details in the modelling (see also the discussion in Sec. 4). We have  $q = g - 1$ , so  $\hat{g} = 5.2$  of Sec. 1 translates into  $\hat{q} = 4.2$ .<sup>8</sup> Furthermore,  $\Gamma = \beta \log_2 \gamma / (2(1 + q))$  due to (2) and (25) together with the fact that  $k = \tau \log_2 \gamma / \Gamma$  by (3) and (23); given  $\hat{\beta} = 5.1 \cdot 10^{-3}$ , this results in  $\hat{\Gamma} = 3.2 \cdot 10^{-3}$  (here and in what follows, we suppress the index  $N$ , since we will work with fixed, finite  $N$  from now on). The resulting fit is reproduced in Fig. 4 (red solid line). In line with Wiser et al. (2013, Fig. 2), we average over all 12 populations, at this point neglecting a certain variability of the parameters between the populations, see their Table S4.

In the light of (22), of the given value  $\hat{\Gamma}$ , and of the fact that  $C \log \gamma \approx 4.7$ , the values of  $\hat{\mu}$  and  $\hat{\varphi}$  cannot both be very small. We therefore now check the limit law against realistic parameter values.

We start by decomposing the compound parameter  $\Gamma$ . Recall from (7) that the *fitness increment due to the first beneficial mutation* is

$$\varphi = \delta(F_0) = \delta(1). \quad (26)$$

This was estimated as 0.1 by Lenski et al. (1991), see also Gerrish and Lenski (1998), and Wiser et al. (2013). For reasons to be explained in Sec. 3.1, however, we work with the somewhat larger value  $\hat{\varphi} = 0.14$ . The mutation probability may then be obtained from (22) as

$$\hat{\mu} = \frac{\hat{\Gamma}}{C \hat{\varphi}^2 \log \gamma} = 0.035. \quad (27)$$

Stochastic simulations of the GKWY model, performed with Algorithm 1 described in the

---

<sup>8</sup>Recall that we denote parameter estimates by a hat to distinguish them from the corresponding theoretical quantities. Figures are rounded to two digits.

Appendix and using the above parameters together with  $N = 5 \cdot 10^6$ , are also shown in Fig. 4. Their mean (over 12 runs) recovers the basic shape of the fitness curve, but systematically underestimates both the limit law and the data. A natural explanation for this is clonal interference, which is absent in the limit under the scaling (10), but leads to loss of mutations for finite  $N$ . This will be taken into account in Sec. 3. But let us note here that the fluctuations in the data are rather larger than those of the simulations; this may well go along with a variability of the parameters between the 12 replicates of the LTEE, which is present in the data, but not in our simulations.

### 3 Including clonal interference

As discussed in Sec. 2, the scaling regime in the GKWY model was such that, with high probability, no new beneficial mutation arrived while the previous one was on its way either to extinction or fixation. As indicated by the simulation results in Fig. 4, also clonal interference should be taken into account. Briefly stated, clonal interference refers to the situation where a second contending mutation appears while the previous one is still on its way to fixation (recall also Footnote 1). It is crucial to keep in mind that, unlike the case without clonal interference considered in Sec. 2, survival of drift may then no longer be identified with fixation; rather, there may be an additional loss of contending mutations due to clonal interference. In particular, the quantity  $\pi$  of (15) must now be addressed as the *probability to survive drift* rather than the fixation probability.

A full analytic treatment of clonal interference is beyond the scope of this paper; in

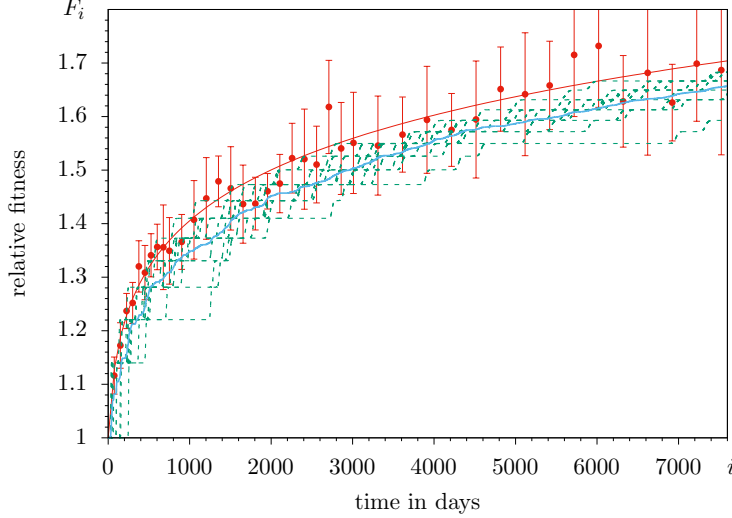


Figure 4: Least-squares fit of the curve (25) to the data in Wiser et al. (2013), and stochastic simulations of finite populations with deterministic beneficial effects. Red bullets: mean empirical relative fitness (averaged over all 12 populations) with error bars as in Fig. 2; solid red line:  $F_i \approx f(\hat{\Gamma}i)$  with parameter values  $\hat{q} = 4.2$  and  $\hat{\Gamma} = 3.2 \cdot 10^{-3}$ ; green lines: 12 individual trajectories  $F_i$  obtained via Cannings simulations with  $N = 5 \cdot 10^6$ ,  $\gamma = 100$ ,  $\hat{\varphi} = 0.14$ , and  $\hat{\mu} = 0.035$ ; light blue line: average over the 12 simulations.

particular, we will not prove a law of large numbers here. Rather, we refine and adapt the heuristics of Gerrish and Lenski (1998), see also Wiser et al. (2013). The heuristics was originally formulated for fitness effects that follow an exponential distribution. We will, however, first consider the deterministic effects as assumed in the GKWY model in Sec. 3.1 and then proceed to random effects from a very general probability distribution in Sec. 3.2.

### 3.1 Deterministic beneficial effects

For the case of deterministic beneficial effects, we will sketch and apply a *thinning heuristics*, as a counterpart of the heuristics of Gerrish and Lenski (1998). Consider the situa-

tion that a second mutation surviving drift appears within the time window  $u(F) := u_N(F)$  of (20) after the appearance of a first mutation (this is more or less while the first mutation has not become dominant yet). Then, with high probability, the second mutation occurs in an individual of relative fitness  $F$  (rather than in an individual of relative fitness  $F + \delta(F)$ ), and therefore belongs to the same fitness class as the first mutant and its offspring. Thus, as far as fitness is concerned, the two mutants (and their offspring) can be considered equivalent. In our heuristics, the occurrence of a second (and also a third, fourth, ...) mutation within the given time window neither speeds up nor decelerates the (order of magnitude of) the time

until the new fitness class is established in the population. So  $u(F)$  plays the role of a *refractory period*, in the sense that the fitness increments carried by contending mutations arriving within this period are lost. The probability that a given increment is *not* lost is determined via the expected waiting time for a (first) contending mutation to appear given the current value  $F$ , which is  $v_1 := 1/(\mu\pi(F))$ , and the expected duration  $v_2 := u(F)$  of the refractory period. Specifically, by (15) and (20), the probability in question is

$$\frac{v_1}{v_1 + v_2} \sim \frac{1}{1 + C\mu \log N}. \quad (28)$$

Under this approximation, the expected per-day increase of the relative fitness, given its current value  $F$ , turns into

$$\mathbb{E}(\Delta F | F) \approx \frac{\mu \pi(F) \delta(F)}{1 + C\mu \log N} \sim \frac{\Gamma}{F^{2q+1}}, \quad (29)$$

where now

$$\Gamma = \frac{C\mu \varphi^2 \log \gamma}{1 + C\mu \log N}, \quad (30)$$

that is, the factor  $\mu$  in (22) is replaced by  $\mu/(1 + C\mu \log N)$ . Now, taking the expectation over  $F$  in (29) yields

$$\mathbb{E}(\Delta F) \approx \Gamma \mathbb{E}\left(\frac{1}{F^{2q+1}}\right) \gtrsim \frac{\Gamma}{(\mathbb{E}(F))^{2q+1}}.$$

Here, the second step is due to Jensen's inequality.<sup>9</sup> Assuming a suitable concentration of the random variables in question around their expectations (which in theory would be justified by a dynamical law of large numbers result such

---

<sup>9</sup>Note that  $1/x^p$  is a convex function of  $x$  for any  $p \geq 1$ .

as the one discussed in Sec. 2, and in practice is a crude way of moment closure) we arrive at the approximation

$$F_{\lfloor \tau/\Gamma \rfloor} \approx \mathbb{E}(F_{\lfloor \tau/\Gamma \rfloor}) \approx f(\tau) \text{ for large } N$$

with  $f$  as in (25). We may, therefore, approximate (as in Fig. 4) the data by the function  $f$ , with the same values  $\hat{q}$  and  $\hat{\Gamma}$  as before. The compound parameter  $\Gamma$ , however, has an internal structure different from the previous one (compare (30) with (22)). Solving (30) for  $\mu$  gives

$$\mu = \frac{\Gamma}{C(\varphi^2 \log \gamma - \Gamma \log N)}; \quad (31)$$

for our current  $\hat{\Gamma}$  and  $\hat{\varphi}$ , this yields  $\hat{\mu} = 0.079$  and thus a better agreement between the simulated mean fitness and the approximating power law (and hence with the data), see Fig. 5. Notably,  $\hat{\mu}$  is of the same order of magnitude as  $1/\log N = 0.15$ ; for an asymptotic analysis as  $N \rightarrow \infty$ , this would imply that the ratio (28) is bounded away from 0. For substantially higher mutation probabilities, the heuristics would break down (Fogle et al. 2008) and a different asymptotic regime would apply (Durrett and Mayberry 2011).

Let us now investigate the remaining discrepancy between the mean of the Cannings simulations and the approximating power law. Since the power law has been obtained via two approximations, namely the thinning heuristics and moment closure, it is interesting to quantify the contributions of these two sources of error. To this end, we simulate the evolution according to the heuristics rather than the Cannings model (see Algorithm 2 in the Appendix). The result is shown in Fig. 6. The simulation mean is very close to that of the



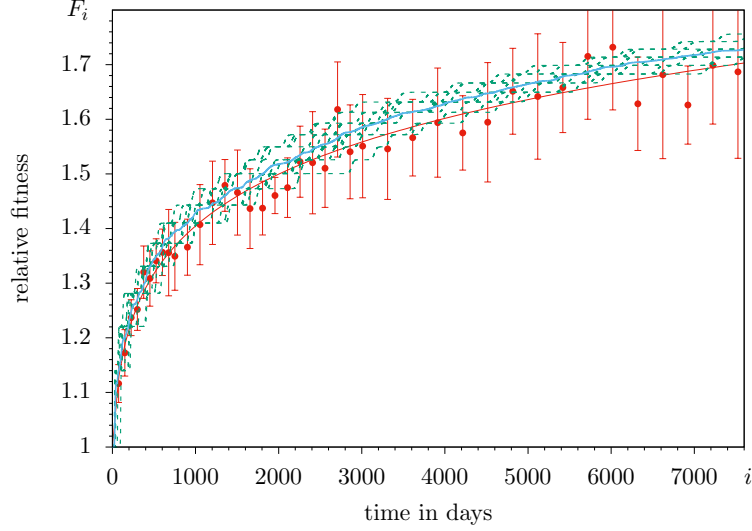


Figure 5: Cannings simulation as in Fig. 4, but with mutation probability  $\hat{\mu} = 0.079$ .

Cannings simulation in Fig. 5. We may conclude that the heuristics approximates the Cannings model very well, at least at the level of the mean values; the discrepancy between the Cannings simulation and the power law should therefore mainly be ascribed to moment closure. Note that the simulation of the heuristics yields smaller fluctuations than that of the Cannings model; this goes along with the fact that the model based on the heuristics contains fewer random elements than the Cannings model.

Let us finally comment on our choice  $\hat{\varphi} = 0.14$ . The denominator of (31) is strictly positive, and hence  $\hat{\mu}$  is finite (and positive) as long as

$$\hat{\varphi} > \sqrt{\frac{\hat{\Gamma} \log N}{\log \gamma}} = 0.10.$$

The existence of such a lower bound on  $\hat{\varphi}$  is plausible since the refractory period poses an

upper bound to the rate of fixation events. Here we work with the value of  $\hat{\varphi} = 0.14$  in order to stay reasonably far away from an undesirable ‘explosion’ of  $\hat{\mu}$ . With this choice, the number of fixed beneficial mutations in the simulation in Fig. 6, averaged over the 12 runs, is 21; this is to be compared with the estimate of 60–110 fixed mutations observed in 50000 generations by Tenaillon et al. (2016), and of 100 fixed mutations observed in 60000 generations by Good et al. (2017), which both include neutral mutations.

### 3.2 Random beneficial effects

Let us now turn to random beneficial effects. To this end, we scale the fitness increments with a positive random variable  $X$  with density  $h$  and expectation  $\mathbb{E}(X) = 1$ . We assume throughout that  $\mathbb{E}(X^2) < \infty$  to ensure that all quantities required in what follows are well-

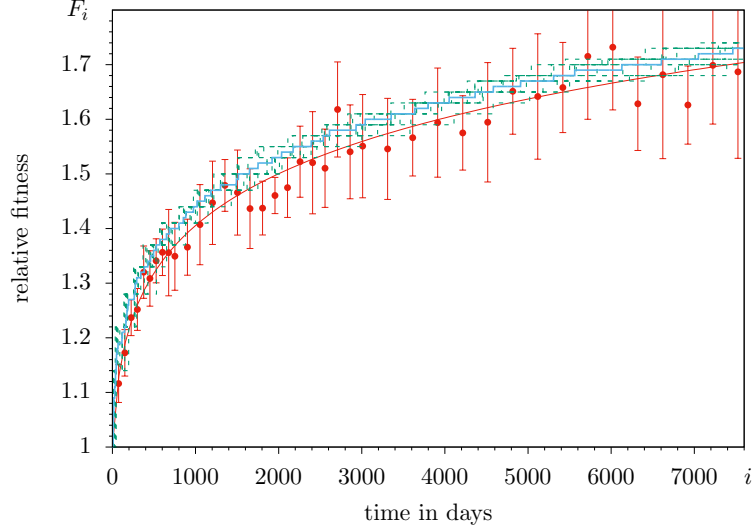


Figure 6: Simulation using heuristics for deterministic increments. Parameters as in Fig. 5. Mean number of clonal interference events: 24; mean number of established beneficial mutations: 21.

defined.

Taking into account the dependence on  $X$ , the quantities in (11)–(13), (15) and (20) turn into

$$\delta(F, X) = X \frac{\varphi}{F^q}, \quad (32a)$$

$$\sigma(F) = \frac{\log \gamma}{F} \text{ (as before),} \quad (32b)$$

$$s(F, X) = \delta(F, X) \sigma(F), \quad (32c)$$

$$\pi(F, X) \approx C s(F, X), \quad (32d)$$

$$u(F, X) = \frac{\log N}{s(F, X)}. \quad (32e)$$

Note first that large  $X$  implies large  $s$  and hence small  $u$  and vice versa; and second that (32d) is an approximation, whereas in (15) we have asymptotic equivalence. The following Poisson picture will be central to our heuristics: The process of *beneficial mutations* with scaled effect  $x$  that arrives at time  $\tau$  has inten-

sity  $\mu d\tau h(x) dx$  with points  $(\tau, x) \in \mathbb{R}_+ \times \mathbb{R}_+$ . And in fitness background  $\approx F$ , we denote by  $\Pi$  the Poisson process of *contending mutations*, i.e. those beneficial mutations that survive drift (but not necessarily go to fixation), which has intensity  $\mu d\tau h(x) \pi(F, x) dx$  on  $\mathbb{R}_+ \times \mathbb{R}_+$ .

We now develop a refined version of the *Gerrish-Lenski heuristics for clonal interference* and adapt it to the context of our model. If, in the fitness background  $\approx F$ , two contending mutations  $(\tau, x)$  and  $(\tau', x')$  appear at  $\tau < \tau' < \tau + u(F, x)$ , then the first one outcompetes (‘kills’) the second one if  $x' \leq x$ , and the second one kills the first one if  $x' > x$ . Thus, neglecting interactions of higher order, given that a contending mutation arrives at  $(\tau, x)$  in the fitness background  $\approx F$ , the probability that it

does not encounter a killer in its past is

$$\begin{aligned} \overleftarrow{\chi}(F, x) := \\ \exp \left( - \int_x^\infty \mu \pi(F, y) u(F, y) h(y) dy \right), \end{aligned} \quad (33)$$

whereas the probability that it does not encounter a killer in its future is

$$\begin{aligned} \overrightarrow{\chi}(F, x) := \\ \exp \left( - u(F, x) \int_x^\infty \mu \pi(F, x') h(x') dx' \right). \end{aligned} \quad (34)$$

Using (32),  $\overleftarrow{\chi}(F, x)$  is approximated by

$$\begin{aligned} \overleftarrow{\psi}(x) := \\ \exp \left( - \mu C \log N \int_x^\infty h(y) dy \right), \end{aligned}$$

whereas  $\overrightarrow{\chi}(F, x)$  is approximated by

$$\begin{aligned} \overrightarrow{\psi}(x) := \\ \exp \left( - \mu \frac{C \log N}{x} \int_x^\infty x' h(x') dx' \right). \end{aligned} \quad (35)$$

Notably, neither  $\overleftarrow{\psi}$  nor  $\overrightarrow{\psi}$  depend on  $F$ . Thus, setting  $\overleftarrow{\chi} := \overleftarrow{\chi} \overrightarrow{\chi}$  and analogously  $\overrightarrow{\psi} := \overleftarrow{\psi} \overrightarrow{\psi}$ , we obtain, as an analogue of (29), the expected (per-day) increase of  $F$ , given the current value of  $F$ , as

$$\begin{aligned} \mathbb{E}(\Delta F | F) \\ \approx \mu \int_0^\infty \delta(F, x) \pi(F, x) \overleftarrow{\chi}(F, x) h(x) dx \\ \approx \frac{C \mu \varphi^2 \log \gamma}{F^{2q+1}} \int_0^\infty x^2 \overleftarrow{\psi}(x) h(x) dx \\ = \frac{\Gamma}{F^{2q+1}}, \end{aligned} \quad (36)$$

where

$$\Gamma := C \mu \varphi^2 \log(\gamma) I(\mu) \quad (37)$$

and  $I(\mu) := \mathbb{E}(\overleftarrow{\psi}(X) X^2)$  is the integral in (36) whose parameter  $\mu$  still has to be determined. Similarly as in Sec. 3.1, the assumption of a suitable concentration of the random variable  $\Delta F$  around its conditional expectation allows us to take (36) into

$$F_{\lfloor \tau / \Gamma \rfloor} \approx \mathbb{E}(F_{\lfloor \tau / \Gamma \rfloor}) \approx f(\tau)$$

with  $f$  as in (25). As in Section 3.1, we will refer to this approximation step as ‘moment closure’. The composite parameter  $\Gamma$  can be estimated from the empirical data in the same way as described at the end of Sec. 2. In order to estimate  $\mu$  and  $\varphi$  with the help of the observed mean fitness increment of the first fixed beneficial mutation (in analogy with (27)), we derive, in our Poisson model, the *expectation of the scaled effect of the first among the contending mutations* (in fitness background  $F = 1$ ) *that is not killed*.

To this end, we consider a sequence of points  $(\mathcal{T}_j, X_j)_{j \geq 1}$  in  $\Pi$  (the Poisson process of contending mutations) that is strictly monotonic increasing in both coordinates and inductively defined as follows.

$(\mathcal{T}_1, X_1)$  is the point in  $\Pi$  with the smallest  $\tau$ -coordinate, and given  $(\mathcal{T}_j, X_j)$ ,  $(\mathcal{T}_{j+1}, X_{j+1})$  is the point in  $\Pi$  with

$$\mathcal{T}_{j+1} = \min\{\tau : (\tau, x) \in \Pi, \tau > \mathcal{T}_j, x > X_j\}.$$

Again we say that  $(\mathcal{T}_{j+1}, X_{j+1})$  kills  $(\mathcal{T}_j, X_j)$ , if  $\mathcal{T}_{j+1} < \mathcal{T}_j + u(X_j)$ .<sup>10</sup> Let

$$Z := \min\{j \geq 1 : \mathcal{T}_{j+1} > \mathcal{T}_j + u(X_j)\},$$

---

<sup>10</sup>As long as we assume  $F = 1$ , we suppress the first argument in the functions defined in (32) for notational convenience.

i.e.  $(\mathcal{T}_Z, X_Z)$  is the earliest among the points  $(\mathcal{T}_j, X_j)$ ,  $j = 1, 2, \dots$ , that is *not killed*. The point  $(\mathcal{T}_Z, X_Z)$  is thus called the (first) *winner*; at time  $\mathcal{T}_Z$ , the relative fitness of the population jumps from 1 to  $1 + \varphi X_Z$ .

Our aim is to find the distribution of the  $x$ -coordinate of the winner,

$$\mathbb{P}(X_Z \in dx), \quad x \geq 0. \quad (38)$$

From elementary properties of Poisson processes we infer that, given  $(\mathcal{T}_j, X_j)$ , the waiting time  $W_{j+1} := \mathcal{T}_{j+1} - \mathcal{T}_j$  is exponentially distributed with parameter

$$\mu \int_{X_j}^{\infty} \pi(y) h(y) dy.$$

Hence

$$\mathbb{P}(W_{j+1} > u(x) \mid X_j = x) = \chi(x),$$

with  $\chi(x) := \vec{\chi}(1, x)$  from (34). Moreover, given  $(\mathcal{T}_j, X_j)$ , the random variables  $W_{j+1}$  and  $X_{j+1}$  are independent, and  $X_{j+1}$  has the conditional density

$$\begin{aligned} \mathbb{P}(X_{j+1} \in dx \mid X_j = y) \\ = \frac{\pi(x) h(x) dx}{\int_y^{\infty} \pi(y') h(y') dy'} =: \rho(x \mid y) dx \end{aligned} \quad (39)$$

for  $x \geq y \geq 0$ . Consequently, the conditional probability that the  $j$ -th of the increasing points is the winner, given that all the previous ones have been killed, is

$$\mathbb{P}(Z = j \mid Z \geq j, X_j = y) = \chi(y),$$

whereas the conditional probability to proceed and see the next killer at  $dx$  is

$$\begin{aligned} \mathbb{P}(Z \geq j+1, X_{j+1} \in dx \mid Z \geq j, X_j = y) \\ = (1 - \chi(y)) \rho(x \mid y) dx. \end{aligned}$$

With  $x_0 := 0$ , this gives the following formula for the joint distribution of  $X_1, \dots, X_Z$  and  $Z$ :

$$\begin{aligned} \mathbb{P}(X_1 \in dx_1, \dots, X_{\ell-1} \in dx_{\ell-1}, X_{\ell} \in dx, Z = \ell) \\ = \prod_{j=1}^{\ell-1} [\rho(x_j \mid x_{j-1}) (1 - \chi(x_j)) dx_j] \\ \cdot \rho(x \mid x_{\ell-1}) \chi(x) dx. \end{aligned} \quad (40)$$

The density  $\mathbb{P}(X_Z \in dx, Z = \ell)$  arises by integrating (40) over  $x_1, \dots, x_{\ell-1}$ , under the constraints  $0 \leq x_1 \leq \dots \leq x_{\ell-1} \leq x$ . Using (39), we see from (40) that

$$\begin{aligned} \mathbb{P}(X_Z \in dx, Z \leq \ell) &= \sum_{k=1}^{\ell} \mathbb{P}(X_Z \in dx, Z = k) \\ &= \pi(x) \chi_{\ell}(x) h(x) dx. \end{aligned} \quad (41)$$

Here  $\chi_{\ell}$  may be read off the product formula (40), plays the role of an additional reweighting factor, and coincides with (34) in the case  $\ell = 1$ . Then, for the density of  $X_Z$  *conditional on*  $Z \leq \ell$ , we obtain

$$\begin{aligned} \mathbb{P}(X_Z \in dx \mid Z \leq \ell) &= \\ &= \frac{\pi(x) \chi_{\ell}(x) h(x) dx}{\int_0^{\infty} \pi(x) \chi_{\ell}(x) h(x) dx}, \end{aligned} \quad (42)$$

which should be very close to (38) for  $\ell$  not too small.

Consequently, with the approximations (32) as well as (35), and  $\psi_{\ell}$  taking the place of  $\chi_{\ell}$  in the approximate analogue of (41),

$$\begin{aligned} \mathbb{E}(\delta(X_Z) \mid Z \leq \ell) &= \varphi \mathbb{E}(X_Z \mid Z \leq \ell) \\ &\approx \varphi \frac{\mathbb{E}(\psi_{\ell}(X) X^2)}{\mathbb{E}(\psi_{\ell}(X) X)} =: \varphi \zeta_{\ell}(\mu). \end{aligned} \quad (43)$$

Note that, under the assumptions on  $X$ ,  $\zeta_{\ell}(\mu)$  (as an approximation of the expectation of the

first scaled beneficial effect that goes to fixation) is parametrised by  $\mu$  (via  $\psi_\ell$ ) and well defined for any  $\mu$ , since  $0 < \psi_\ell \leq 1$ .

Then, again for  $\ell$  not too small, the left-hand side of (43) may be a good approximation for the observed value of the mean fitness increment due to the first fixed beneficial mutation, which we denote by  $\mathfrak{d}_1$ . Indeed, (37) together with (43) renders the system of equations

$$\frac{\mu I(\mu)}{(\zeta_\ell(\mu))^2} = \frac{\Gamma}{C \mathfrak{d}_1^2 \log \gamma}, \quad (44a)$$

$$\varphi = \frac{\mathfrak{d}_1}{\zeta_\ell(\mu)} \quad (44b)$$

where  $\mu$ , as the solution of (44a), determines  $\varphi$  via (44b). We will carry out this program with  $\ell = 3$  for two special choices of  $h$  in the remainder of this section. Let us anticipate that numerical evaluations show that the left-hand side of (44a) is monotone increasing in  $\mu$  on  $[0, 1]$  for both choices. For (44a) to have a solution, it is therefore required that

$$\mathfrak{d}_1 > \sqrt{\frac{\Gamma}{C \log \gamma I(1)}} \zeta_3(1), \quad (44c)$$

which will serve as a lower bound for the estimate  $\widehat{\mathfrak{d}}_1$ .

The analysis so far allows to conclude that, as long as the above described approximation may be relied on, the *mean fitness curve* observed by Wisner et al. (2013) *can be described by any distribution of fitness effects*, provided the mutation probability is chosen according to (44a) (and provided that (44a) has a solution). In particular, the *epistasis parameter*  $q$  is *not affected by the distribution* of  $X$ .

**Exponentially distributed beneficial effects.** For definiteness, we now turn to ran-

dom beneficial effects where  $X$  follows  $\text{Exp}(1)$ , the exponential distribution with parameter 1. This is the canonical choice since strongly-beneficial mutations appear to be exponentially distributed; the experimental evidence is reviewed by Eyre-Walker and Keightley (2007), and it confirms theoretical predictions (Gillespie 1984; Orr 2003). The distribution of slightly-beneficial mutations is less well known, but these mutations contribute little to the adaptive process.

Thus, by (44), we have  $\widehat{\mu} = 0.11$  and hence  $\widehat{\varphi} = 0.069$  for  $\widehat{\mathfrak{d}}_1 = 0.20 \gtrapprox 0.16$  for this choice of the distribution of  $X$ . Fig. 7 shows the corresponding Cannings simulations, and Fig. 8 displays the simulations according to the heuristics. The agreement of the simulation mean with the approximating power law is now nearly perfect. The fluctuations, however, are smaller in the simulations than in the experiment. As argued in Sec. 2 in the context of the first reality check, this may be explained by the constant parameters assumed by the model, whereas parameters do vary across replicate populations in the experiment.

Let us also mention the degree of polymorphism observed in the Cannings simulations of Fig. 7. Counting a type as ‘present’ if its frequency is at least 20%, it turns out that, on average, the population is monomorphic on 89.1% of the days; it contains two types on 10.6% of the days, and three types on 0.3% of the days. Thus, in the finite system, some polymorphism is present, but it is not abundant. Recall that our model does not consider neutral mutations, and thus the low level of (fitness) polymorphism observed in the simulations does not contradict the high level of genetic diversity observed in experiments (Tenaillon et al. 2016).

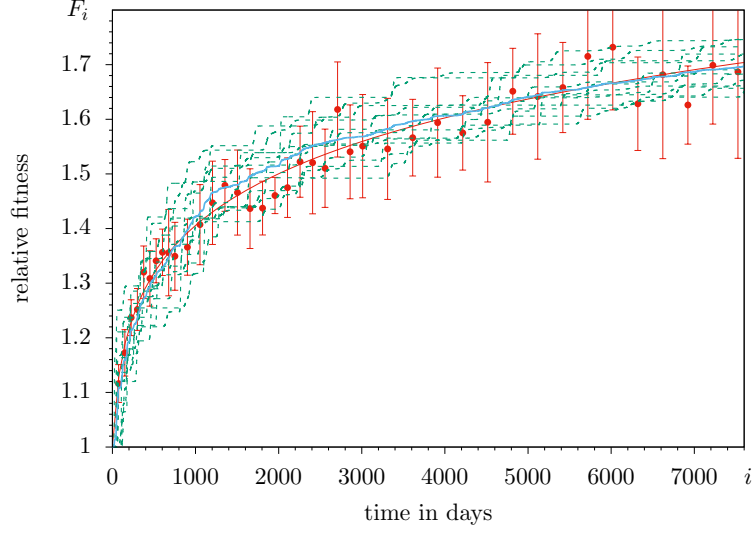


Figure 7: Simulations of the Cannings model with  $X$  following  $\text{Exp}(1)$  and parameters  $\hat{\varphi} = 0.069$ , and mutation probability  $\hat{\mu} = 0.11$ .

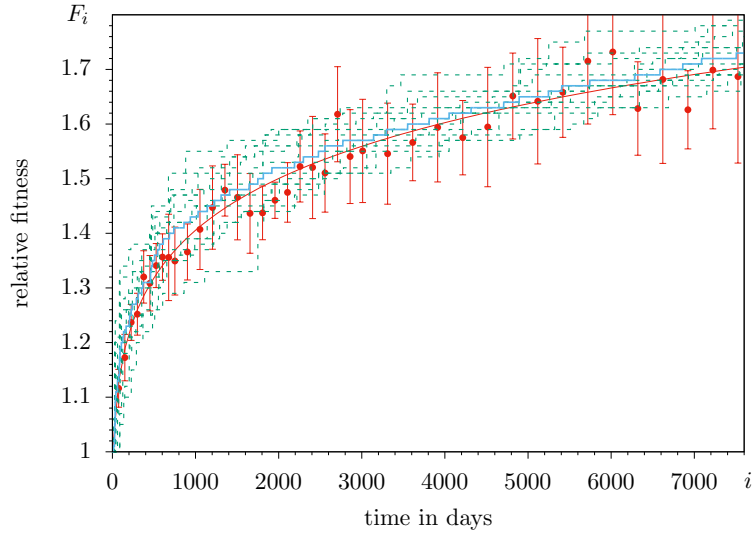


Figure 8: Simulations using Gerrish-Lenski heuristics with  $X$  following  $\text{Exp}(1)$  and parameters as in Fig. 7. Mean number of clonal interference events with  $x' \leq x$ : 7.9; mean number of clonal interference events with  $x' > x$ : 7.8; mean number of established beneficial mutations: 23.

**Beneficial effects with a Pareto distribution.** As argued already, the exponential distribution seems to be the most realistic choice for beneficial mutation effects. The theory developed above, however, holds for arbitrary probability distributions on the positive half axis that have expectation 1 and a finite second moment. Furthermore, the analysis of the heuristics indicates that the results are, in fact, independent of the distribution, provided the compound parameter  $\Gamma$  is interpreted in the appropriate way. It is therefore interesting to explore whether this conclusion may be verified by simulations. In order to push our conjecture to the limits, we choose  $X$  distributed according to a (*shifted*) *Pareto distribution* (see Feller (1971, Ch. II.4) or Stuart and Ord (1994, Ex. 2.19)) with shape parameter  $\lambda$  as given by the density

$$h(x) = \begin{cases} 0, & x < 0 \\ \frac{\lambda}{\lambda-1} \left( \frac{\lambda-1}{x+(\lambda-1)} \right)^{\lambda+1}, & x \geq 0. \end{cases} \quad (45)$$

The parameter  $\lambda \geq 0$  controls which of the moments of  $X$  exist. For  $0 < \lambda \leq 1$ , the expectation is infinite; for  $1 < \lambda < 2$ , the expectation is 1 but the second moment is infinite; for  $2 < \lambda \leq 3$ ,  $\mathbb{E}(X) = 1$  and  $\mathbb{E}(X^2) = 2(\lambda-1)/(\lambda-2)$  but the third moment is infinite; and similarly for larger  $\lambda$ . We work with  $\lambda = 2.5$  here; this implies that there is no restriction in applying our analysis.

Proceeding in analogy with the case of exponentially distributed beneficial effects, we simulate both the Cannings model and the heuristics and compare them with the approximating power law. The result is shown in Figs. 9 and 10. As was to be expected, the mean is still well described by the approximating power law, but the fluctuations are enhanced rela-

tive to the case of the exponential distribution (note that now  $\mathbb{E}(X^2) = 6$  in contrast to  $\mathbb{E}(X^2) = 2$  in the case of  $\text{Exp}(1)$ , and thus, by (44), we have  $\hat{\mu} = 0.37$  and hence  $\hat{\varphi} = 0.020$  for  $\hat{\mathfrak{d}}_1 = 0.12 \gtrapprox 0.10$ ). Compared to the experiment, the fluctuations are unrealistically large; an effect distribution with high variance therefore does not appear to be close to the truth.

## 4 Discussion

We have, so far, postponed a detailed comparison with the model and the results of Wiser et al. (2013). We now have everything at hand to do so.

**Modelling aspects.** Both the WRL model and ours lead to power laws, (2) and (25), which are of the same form. But the modelling assumptions differ in relevant details, with consequences for the interpretation of the parameters. Here and below we use a tilde to distinguish the quantities belonging to the WRL model from our corresponding quantities.

The main difference is that Wiser et al. (2013) describe the experiment with a discrete generation scheme given by  $\log_2 \gamma$  ( $\approx 6.6$ ) doublings during one daily growth phase, see Fig. 11. This neglects the variability that comes from a continuous-time intraday reproduction mechanism, and affects the WRL analogue to our formula (15) for the probability to survive drift. The latter is stated in (S1) of their Supplementary Text, reads

$$\tilde{\pi} = \tilde{\pi}(\tilde{s}) = 4\tilde{s}, \quad (46)$$

and relies on Gerrish and Lenski (1998), Appendix 1. In line with the generation scheme of Fig. 11,  $\tilde{s}$  is the selective advantage in each

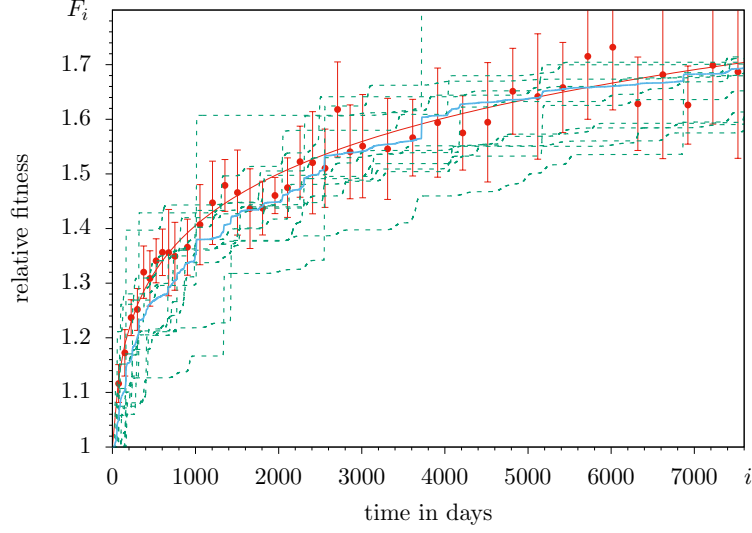


Figure 9: Simulations of the Cannings model with  $X$  following the (shifted) Pareto distribution with density  $h$  of (45). Parameters:  $\lambda = 2.5$ ,  $\hat{\varphi} = 0.020$ , and  $\hat{\mu} = 0.37$ .

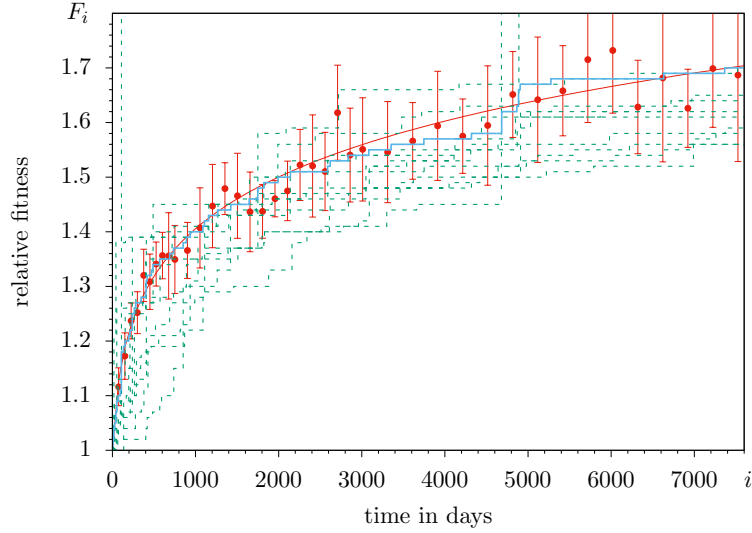


Figure 10: Simulations using Gerrish-Lenski heuristics with  $X$  following the (shifted) Pareto distribution and parameters as in Fig. 9. Mean number of clonal interference events with  $x' \leq x$ : 13; mean number of clonal interference events with  $x' > x$ : 9.1; mean number of established beneficial mutations: 21.



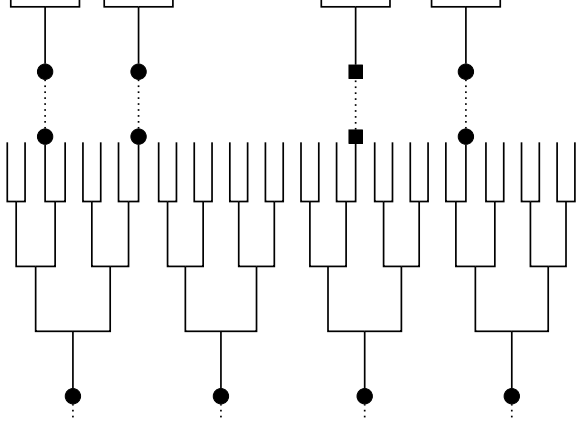


Figure 11: Synchronous growth model as used in Gerrish and Lenski (1998), with equally-sized clones at the end of the day (here,  $\gamma = 8$ ); compare Fig. 1.

of the  $\log_2 \gamma$  generations per day. At the end of the day, the population has increased from size  $N$  to size  $\gamma N$  and consists of  $N$  clones, each of size  $\gamma$ . A sampling of  $N$  individuals without replacement thus leads to a pair coalescence probability of  $(\gamma - 1)/(\gamma N)$ , and hence to an offspring variance per day of

$$\tilde{v} \sim \frac{\gamma - 1}{\gamma}; \quad (47)$$

note the factor of 2 between  $\tilde{v}$  and our  $v$  in (16), which comes from a size-biasing effect due to the sampling from clones of random size.

Since  $\tilde{s}$  is related to one ‘doubling generation’, the selective advantage *per day* is

$$\tilde{s}_d \approx \tilde{s} \log_2 \gamma. \quad (48)$$

Now, Haldane’s formula (17) related to the daily rhythm gives

$$\tilde{\pi} \approx \frac{\tilde{s}_d}{\tilde{v}_d/2},$$

and, with (46), this yields a per-day offspring variance  $\tilde{v}_d \approx \log_2 \gamma$ , which differs significantly from  $\tilde{v}$  in (47) for  $\gamma = 100$ . Thus, we see that the ansatz of Wiser et al. (2013) combined with Gerrish and Lenski (1998) leads to an ambiguously defined offspring variance per day.

Moreover, at the end of the Materials and Methods section in the Supplement, Wiser et al. (2013) relate the difference between the new and the old relative fitness to the (per generation) selective advantage of a mutant as follows:

$$w_{\text{new}} = w(1 + \tilde{s}) \quad (49)$$

with  $\tilde{s}$  from (46). Here

$$w = w_i = \frac{\log \tilde{a}}{\log \tilde{b}}, \quad (50)$$

with the growth factors  $\tilde{a} = Y_i(T_i)/Y_i(0)$  and  $\tilde{b} = Y_0(T_i)/Y_0(0)$  as in (1). They are not explicit about an intraday growth model, so one should think of  $Y_i(0)$ ,  $Y_0(0)$ ,  $Y_i(T_i)$  and  $Y_0(T_i)$  as the numbers of individuals at the beginning and the end of the competition experiment. For a consistent definition of the selective advantage per day, it is inevitable to use the growth factors  $a_{\text{new}}$  and  $a$  related to one day; then, according to (14), one has

$$s_d = \frac{a_{\text{new}} - a}{a} \sim \log \frac{a_{\text{new}}}{a}. \quad (51)$$

In principle,  $a$  may (and will) differ from the  $\tilde{a}$  in the definition of  $w$ . At least in a model with intraday exponential growth, however, the definition of  $w$  in (50) becomes independent of  $T_i$ ; we may (and will) therefore use the growth factors  $a = Y_i(\sigma_i)/Y_i(0)$  and  $b = Y_0(\sigma_i)/Y_0(0)$  instead of  $\tilde{a}$  and  $\tilde{b}$  in (50). Then (50) implies

$$\frac{w_{\text{new}}}{w} = \frac{1}{\log a} \left( \log \left( \frac{a_{\text{new}}}{a} \right) + \log a \right), \quad (52)$$

which by (51) yields

$$w_{\text{new}} = w \left( 1 + \frac{s_d}{\log a} \right), \quad (53)$$

or equivalently, using (50) again,

$$w_{\text{new}} - w = \frac{s_d}{\log b}. \quad (54)$$

Under the assumption of an intraday exponential growth we have (as long as the populations are nearly homogeneous):

$$a \approx e^{r\sigma}, \quad b \approx e^\sigma, \quad w \approx r, \quad r\sigma \approx \log \gamma. \quad (55)$$

Thus (54) translates into

$$s_d \approx \frac{1}{r} (r_{\text{new}} - r) \log \gamma, \quad (56)$$

which also results from combining (12) and (13) and equating  $F$  and  $r$ . This shows that the runtime effect discussed in Sec. 2 is already implicit in the definition (50) of  $w$  as the ratio of logarithms of growth factors, as soon as one uses a model with intraday exponential growth. Let us emphasise again that this runtime effect is a consequence of the design of Lenski's experiment; it would be absent in a variant of the experiment in which sampling occurs at a given fixed time before the onset of the starvation phase.

Furthermore, comparing (53) with (49) and using (55) gives

$$s_d = \tilde{s} \log a \approx \tilde{s} \log \gamma.$$

Comparing with (48), this shows that

$$s_d = \frac{\log \gamma}{\log_2 \gamma} \tilde{s}_d,$$

which points to a certain inconsistency inherent in  $\tilde{s}_d$ .

Another issue worth to compare is the interpretation of *diminishing returns epistasis*, and the corresponding translation between the exponent  $g$  in the WRL model and the exponent  $q$  in ours. Formula (S1) of Wiser et al. (2013) says that the multiplicative effect on  $r$  has expected size  $1/\alpha$ ; this corresponds to an additive effect on  $r$  of expected size  $\delta := r/\alpha$ . Thus, the ansatz (11) translates into

$$\frac{1}{\alpha} = \frac{\varphi}{r^{q+1}}.$$

On the other hand, formula (S9) in Wiser et al. (2013) says that

$$\alpha = c e^{g \log r},$$

which implies that  $g = q + 1$ . The choice  $g = 1$  in the WRL model (or equivalently,  $q = 0$  in ours, cf. (2) and (25)) corresponds to *additive* increments on the Malthusian fitness that do not depend on the current value of the latter, see (11). It is this case of constant additive increments which may be appropriately addressed as the *absence of epistasis*. More precisely, in *continuous time* (as considered here for the intraday dynamics), additive fitness increments correspond to independent action of mutations and hence to absence of epistasis (Fisher (1918); Bürger (2000, pp. 48 and 74)); in *discrete time*, the same would be true of multiplicative increments. Consequently,  $q = g - 1$  can be seen as an exponent describing the effect of epistasis. With this interpretation, a (slight) concavity of the mean fitness curve is caused by the runtime effect (and hence by the design of the experiment) even in the absence of epistasis. This fact, which is due to the runtime effect, is sometimes overlooked when interpreting the mean fitness curve; see, for example, Good and Desai (2015).

A substantial part of the derivations of Wiser et al. (2013) deals with incorporating the Gerrish-Lenski heuristics for *clonal interference* into their model. The fact that they work with multiplicative fitness increments and various approximations complicates the translation between the time-scaling constant in their power law (S16) (that we subsume as  $\beta$  in (2)) and our time-scaling constant  $\Gamma$  (see (25) and (37)). We refrain from pursuing the details here; but let us emphasise that (32) together with the calibrations discussed in Sec. 3.2 applies to arbitrary random (additive) fitness effects with finite second moments.

**Analytic and simulation results.** We have presented three lines of results. First, rigorous results for the relative mean fitness in terms of a law of large numbers in the limit  $N \rightarrow \infty$  for deterministic beneficial effects in a regime of weak mutation and moderately strong selection. Second, we have derived transparent analytic expressions for the *expected* mean fitness in a finite- $N$  system by means of heuristics of Gerrish-Lenski type and a moment closure approximation (which is also used by Wiser et al. (2013)). The beneficial effects may be either deterministic (and then require a specific thinning heuristics), or random with an arbitrary density. In the latter case we have developed a refinement of the original Gerrish-Lenski heuristics. Briefly stated, this refinement does not only consider the thinning factor (34) coming from *future* interfering mutations, but also the thinning factor (33) coming from *past* ones. This makes the heuristics consistent with its verbal description, which says that ‘if two contending mutations appear within the time required to become dominant in the population,

then the fitter one wins.’ A refinement that also includes thinning due to past competitors was suggested by Gerrish (2001), but contains less detail; in particular, it does not allow conclusions about the distribution of the effects of the ‘winning’ mutations.

For reasons of calibration, we have indeed established an approximate analytic expression (43) for the expected scaled effect of the first beneficial mutation that goes to fixation. This introduces a *size bias* into the distribution of beneficial effects (see (42)), similar to the descriptions by Rozen et al. (2001) and Wiser et al. (2013) in the case of the exponential distribution.

As it turned out, the analytic expressions are *robust*. In particular, the estimate of  $q$  is neither affected by clonal interference nor by the choice of the distribution. What changes is the internal structure of the compound parameter  $\Gamma$ , but for any given estimate  $\hat{\Gamma}$ , the mutation probability and scaling of beneficial effects may be arranged appropriately (provided  $X$  has second moments). The deviations from  $q = 0$  are a signal of diminishing returns epistasis; at this point, let us emphasise again that the approximating curve of the mean relative fitness is (slightly) concave even for  $q = 0$  (due to the runtime effect). By any means, the pronounced concavity in the curve approximating the LTEE data (with its estimated  $\hat{q} = 4.2$ ) gives strong evidence for diminishing returns epistasis, in line with the conclusions of previous investigations (Wiser et al. 2013; Good and Desai 2015; Wünsche et al. 2017). We would like to emphasise, however, that our goal here was not to find the ‘best’ (or even the ‘true’) increment function; rather, the choice (11) was made for the sake of comparison with Wiser et al. (2013), while the GKWY model in fact allows for arbi-

trary increment functions.

Our third line of investigations is a simulation study both of the Cannings model and the approximating heuristics. Here it turned out that the heuristics approximates the Cannings model very well (it might be improved even further by taking into account the refined heuristics of Gerrish (2001) and Rozen et al. (2001)). This suggests that the discrepancy between the (mean of the) Cannings simulations and the approximating power law is mainly due to moment closure. The simulations show that this deviation is moderate for deterministic increments, minute for exponential increments, and hard to quantify for Pareto increments due to the large fluctuations.

## Appendix: Simulation algorithms

Let us briefly describe the two algorithms we have used to simulate our model. Before we come to the details, let us say a few words about notation and strategy. We will throughout use the framework (32), which reduces to (11)–(13), (15) and (20) in the case of deterministic beneficial effects, where  $X \equiv 1$ , that is, the distribution of  $X$  is a point measure on 1. (But note that, in Sec. 3.2, we assume that  $X$  has a density; this implies that any two realisations of  $X$  are different with probability 1, so that there is a clear ‘winner’ in the Gerrish-Lenski heuristics. The analysis of Sec. 3.2 therefore does not carry over to the deterministic case.) *Curly* symbols indicate *sets* of values, whereas *bold* symbols indicate *lists* and  $\bullet^{(k)}$  their  $k$ -th element. By slight abuse of notation, we denote by  $\delta$  ( $\delta^\dagger$ ) the increment of relative fitness (32a) for the current (previous) mutation.

**Algorithm 1** It performs an individual-based simulation of the Cannings model with selection, as formulated in Sec. 2. Its iterations are based on real-world days  $i$ . The algorithm keeps track of the sizes  $\mathcal{N}_j$  of the classes (or subpopulations) of individuals that have reproduction rate  $\mathcal{R}_j$ ,  $j \geq 1$ . As long as  $n_{\text{typ}}$ , the number of different reproduction rates in the population, equals 1, the population is homogeneous, so that the intraday growth and subsequent sampling do not change the current state. If  $n_{\text{typ}} > 1$ , we use the fact that the clone size at time  $\sigma$  in a Yule process with branching rate  $\mathcal{R}_j$  started by a single individual is 1 plus a random variable that follows  $\text{Geo}(e^{-\mathcal{R}_j\sigma})$ , the geometric distribution<sup>11</sup> with parameter  $e^{-\mathcal{R}_j\sigma}$  (cf. Feller (1968, Ch. XVII.3) or Durrett (2008, Ch. 1.3.3)). The size of the corresponding subpopulation at time  $\sigma$  is then  $\mathcal{N}_j$  plus the sum of  $\mathcal{N}_j$  independent copies of the geometric random variable. This sum follows  $\text{NB}(\mathcal{N}_j, e^{-\mathcal{R}_j\sigma})$ , the negative binomial distribution with parameters  $\mathcal{N}_j$  and  $e^{-\mathcal{R}_j\sigma}$ , cf. Feller (1968, Ch. VI.8) or Stuart and Ord (1994, pp. 168/169). The only point where each individual must be treated separately is the sampling step, where  $N = 5 \cdot 10^6$  new founder individuals are drawn without replacement from the  $\approx 5 \cdot 10^8$  descendants. After the sampling, the number of mutation events is drawn from  $\text{Poi}(\hat{\mu})$ , the Poisson distribution with parameter  $\hat{\mu}$  (line 13). The affected individuals are then chosen *uniformly without replacement* from among the  $N$  new founders.

**Algorithm 2** It unifies the two versions of the thinning heuristics of Sec. 3. We now

---

<sup>11</sup>We take  $\text{Geo}(p)$  as the distribution of the numbers of failures before the first success in a coin tossing with success probability  $p$ .

only keep track of substitutions that effectively lead to an increase of the relative fitness, and thus have a homogeneous population in every iteration  $k$ . The number  $k$  counts the fixation events, and the vector  $\boldsymbol{\iota}$  holds the times at which they occur. More precisely, mutations appear after waiting times  $\Delta_{\iota}$  following  $\text{Exp}(\hat{\mu})$  (approximating the discrete  $\text{Geo}(\hat{\mu})$ -distribution). For every such mutation, it is decided whether or not it survives drift by drawing a Bernoulli random variable with success probability  $\pi$  according to (32d) (line 13). If the mutation survives, it is queried whether it survives clonal interference. We simulate this by first adding the increment  $\delta^{\uparrow}$  due to a ‘first’ mutation to the mean fitness, and then adding the additional increment  $\delta - \delta^{\uparrow}$  due to the ‘second’ mutation if it outcompetes the former. For the choice  $X \equiv 1$ , this means that the first out of two competing mutations wins; the case of **A fitter mutation appeared** in line 7 can never occur for deterministic increments.

For the sake of completeness, the parameter combinations for the simulations in this paper are summarised in Tab. 1.

---

**Algorithm 1:** Simulating Lenski's experiment (Cannings model)

---

**Input:** User chosen density law of  $X$  and parameters  $\iota_{\max}, \hat{q}, \hat{\mu}, \hat{\varphi}$ .

```
1 Initialise  $k = 0, \sigma = 1, n_{\text{typ}} = 1, n_{\text{mut}} = 0, \mathcal{R} = \{1\}, \mathcal{N} = \{N\}$ .
2 while  $k < \iota_{\max}$  do
    // Length of intraday growth time
3   Solve (6), i.e.  $\sum_{j=1}^{n_{\text{typ}}} \mathcal{N}_j e^{\mathcal{R}_j \sigma} = \gamma N$ , to obtain  $\sigma$ .
4   Set  $\mathbf{F}^{(k)}$  according to (8).
5   if  $n_{\text{typ}} > 1$  then
       // Intraday population growth
6        $n_{\text{des}} \leftarrow 0$ .
7       for  $j = 1, \dots, n_{\text{typ}}$  do
8           Draw  $D \sim \text{NB}(\mathcal{N}_j, e^{-\mathcal{R}_j \sigma})$  and set  $n_{\text{des}} \leftarrow n_{\text{des}} + \mathcal{N}_j + D$ .
       // Interday sampling
9       Draw sample  $\{j_1, \dots, j_N\}$  without replacement from  $\{1, \dots, n_{\text{des}}\}$  and set
        $\mathcal{N} = \{\mathcal{N}_1, \dots, \mathcal{N}_{n_{\text{typ}}}\}$  accordingly.
10      for  $j = 1, \dots, n_{\text{typ}}$  do
11          if  $\mathcal{N}_j = 0$  then
12              Remove type  $j$  and set  $n_{\text{typ}} \leftarrow n_{\text{typ}} - 1$ .
       // Mutation
13      Draw  $n_{\text{mut}} \sim \text{Poi}(\hat{\mu})$  and set  $n_{\text{typ}} \leftarrow n_{\text{typ}} + n_{\text{mut}}$ .
14      if  $n_{\text{mut}} > 0$  then
15          Draw sample  $\{i_1, \dots, i_{n_{\text{mut}}}\}$  without replacement from  $\{1, \dots, N\}$ .
16          for  $j = 1, \dots, n_{\text{mut}}$  do
17               $\mathcal{N}_{i_j} \leftarrow \mathcal{N}_{i_j} - 1$  and  $\mathcal{N} \leftarrow \mathcal{N} \cup \{1\}$ .
18              Draw  $X$  and set  $\mathcal{R} \leftarrow \mathcal{R} \cup \{\mathcal{R}_{i_j} + \delta(\mathcal{R}_{i_j}, X)\}$  acc. to (32a).
19              if  $\mathcal{N}_{i_j} = 0$  then
20                  Remove type  $i_j$  and set  $n_{\text{typ}} \leftarrow n_{\text{typ}} - 1$ .
21       $k \leftarrow k + 1$ .
22 return  $\mathbf{F}$ .
```

---

---

**Algorithm 2:** Simulating Lenski's experiment (thinning heuristics)

---

**Input:** User chosen law of  $X$  and parameters  $\iota_{\max}, \hat{q}, \hat{\mu}, \hat{\varphi}$ .

```

1 Initialise  $k = 0, \iota = 0, \delta = \delta^\uparrow = 0, \boldsymbol{\iota}^{(0)} = 0, \mathbf{F}^{(0)} = 1$ .
2 while not terminated, i.e.  $\boldsymbol{\iota}^{(k)} + \iota \leq \iota_{\max} \wedge k \leq k_{\max}$  do
    // Not within refractory period according to (32e), (32c), (32b)
3   if  $\iota > \log(N)/(\delta^\uparrow \sigma(\mathbf{F}^{(k)}))$  then
       // Beneficial mutant becomes fixed unrivalled
4        $(\boldsymbol{\iota}^{(k+1)}, \mathbf{F}^{(k+1)}) \leftarrow (\boldsymbol{\iota}^{(k)} + \iota, \mathbf{F}^{(k)} + \delta)$ .
5        $(\iota, k, \delta^\uparrow) \leftarrow (0, k + 1, \delta)$ .
6   else
       // A fitter mutation appeared
7       if  $\delta > \delta^\uparrow$  then
8            $(\boldsymbol{\iota}^{(k+1)}, \mathbf{F}^{(k+1)}) \leftarrow (\boldsymbol{\iota}^{(k)} + \iota, \mathbf{F}^{(k)} + \delta - \delta^\uparrow)$ .
9            $(\iota, k, \delta^\uparrow) \leftarrow (0, k + 1, \delta)$ .
       // Occurrence of a next mutant to become dominant
10      do
11          Draw  $X$  and set  $\delta \leftarrow \hat{\varphi} X(\mathbf{F}^{(k)})^{-\hat{q}}$  according to (32a).
12          Draw  $\Delta_\iota$  following  $\text{Exp}(\hat{\mu})$  and set  $\iota \leftarrow \iota + \Delta_\iota$ .
13      while  $S$  following  $\text{Ber}(C\delta\sigma(\mathbf{F}^{(k)}))$  is unsuccessful according to (32d)
14 return  $(\iota, \mathbf{F})$ .
```

---

Law of $X$	$\iota_{\max}$	$\hat{q}$	$(\hat{\mathfrak{d}}_1)$	$\hat{\mu}$	$\hat{\varphi}$	Algo. 1	Algo. 2
$\equiv 1$	7600	4.2	(0.14)	0.035	0.140	Fig. 4	
$\equiv 1$	7600	4.2	(0.14)	0.079	0.140	Fig. 5	Fig. 6
Exp(1)	7600	4.2	(0.20)	0.106	0.069	Fig. 7	Fig. 8
shifted Pareto, $\lambda = 2.5$ , cf. (45)	7600	4.2	(0.12)	0.373	0.020	Fig. 9	Fig. 10

Table 1: Summary of parameter values for simulations. The population size and the dilution factor have been fixed as  $N = 5 \cdot 10^6$  and  $\gamma = 100$  throughout.



## Acknowledgements

It is our pleasure to thank Phil Gerrish for valuable hints and comments on the manuscript. The paper also profited from discussions with Jason Schweinsberg about the WRL model and its analysis; he further pointed us to a strategy to relax the lower bound on the order of the selection strength in González Casanova et al. (2016), see the discussion in the paragraph *Scaling regime* in Sec. 2. Last not least, we thank Richard Lenski for stimulating discussions. This project received financial support from Deutsche Forschungsgemeinschaft (German Research Foundation, DFG) via Priority Programme SPP 1590 *Probabilistic Structures in Evolution*, grants no. BA 2469/5-2 and WA 967/4-2.

## References

- J.E. Barrick, D. S. Yu, S. H. Yoon, H. Jeong, T. K. Oh, D. Schneider, R. E. Lenski, and J. F. Kim, Genome evolution and adaptation in a long-term experiment with *Escherichia coli*, *Nature* **461** (2009), 1243–1247.
- R. Bürger, *The Mathematical Theory of Selection, Recombination, and Mutation*, Wiley, Chichester, 2000.
- L.M. Chevin, On measuring selection in experimental evolution, *Biology Letters* **7** (2011), 210–213.
- M.M. Desai and D. S. Fisher DS, Beneficial mutation-selection balance and the effect of linkage on positive selection, *Genetics* **176** (2007), 1759–1798.
- R. Durrett, *Probability Models for DNA Sequence Evolution*, 2nd ed., Springer, New York, 2008.
- R. Durrett and J. Mayberry, Travelling waves of selective sweeps, *Ann. Appl. Prob.* **21** (2011), 699–744.
- W.J. Ewens, *Mathematical Population Genetics*, 2nd ed., Springer, New York, 2004.
- A. Eyre-Walker and P.D. Keightley, The distribution of fitness effects of new mutations, *Nature Reviews Genetics* **8** (2007), 610–618.
- W. Feller, *An Introduction to Probability Theory and its Applications*, Vol. I, 3rd ed., Wiley, New York, 1968.
- W. Feller, *An Introduction to Probability Theory and its Applications*, Vol. II, 2nd ed., Wiley, New York, 1971.
- R. Fisher, The correlation between relatives on the supposition of Mendelian inheritance, *Phil. Trans. R. Soc. Edinburgh* **52** (1918), 399–433.
- C.A. Fogle, J.L. Nagle, and M.M. Desai, Clonal interference, multiple mutations and adaptation in large asexual populations, *Genetics* **180** (2008), 2163–2173.
- H.O. Georgii, *Stochastics*, 2nd ed., De Gruyter, Berlin, 2013.
- P.J. Gerrish and R.E. Lenski, The fate of competing beneficial mutations in an asexual population, *Genetica* **102/103** (1998), 127–144.
- P.J. Gerrish, The rhytm of microbial adaptations, *Nature* **413** (2001), 299–302.

- J.H. Gillespie, Molecular evolution over the mutational landscape, *Evolution* **38** (1984), 1116–1129.
- A. González Casanova, N. Kurt, A. Wakolbinger, and L. Yuan, An individual-based model for the Lenski experiment, and the deceleration of the relative fitness, *Stoch. Proc. Appl.* **126** (2016), 2211–2252.
- B.H. Good and M.M. Desai, The impact of macroscopic epistasis on long-term evolutionary dynamics, *Genetics* **199** (2015), 177–190.
- B.H. Good, M.J. McDonald, J.E. Barrick, R.E. Lenski, and M.M. Desai, The dynamics of molecular evolution over 60,000 generations, *Nature* **551** (2017), 45–50.
- D. Graur and W.-H. Li, *Fundamentals of Molecular Evolution*, 2nd ed., Sinauer, Sunderland, MA (2000).
- J.S. LeClair and L.M. Wahl, The impact of population bottlenecks on microbial adaptation, *J. Stat. Phys.* **172** (2017), 114–125.
- R. Lenski, M.R. Rose, S. Simpson, and Tadler, Long term experimental evolution in *Escherichia coli* I. Adaptation and divergence during 2000 generations, *Amer. Nat.* **138** (1991), 1315–1341.
- R. E. Lenski and M. Travisano, Dynamics of adaptation and diversification: a 10,000-generation experiment with bacterial populations, *Proc. Natl. Acad. Sci. U.S.A.* **91** (1994), 6808–6814.
- H.A. Orr, The distribution of fitness effects among beneficial mutations, *Genetics* **163**(2003), 1519–1526.
- S.-C. Park, J. Krug, Clonal interference in large populations, *Proc. Natl. Acad. Sci. U.S.A.* **104** (2007), 18135–18140.
- Z. Patwa and L.M. Wahl, The fixation probability of beneficial mutations, *J. R. Soc. Interface* **5** (2008), 1279–1289.
- P. Phillips, S. Otto, and M. Whitlock, Beyond the average: the evolutionary importance of gene interactions and variability of epistatic effects, in “Epistasis and the Evolutionary Process” (J. Wolf, E. Brodie, and M. Wade, Eds.), 2000, pp. 20–38, Oxford University Press, Oxford.
- D.E. Rozen, J.A.G.M. de Visser, and P.J. Gerish, Fitness effects of fixed beneficial mutations in microbial populations, *Current Biology* **12** (2002), 1040–1045.
- R. Sanjuán, Mutational fitness effects in RNA and single-stranded DNA viruses: common patterns revealed by site-directed mutagenesis studies, *Phil. Trans. R. Soc. B* **365** (2010), 1975–1982.
- A. Stuart and K.J. Ord, *Kendalls Advanced Theory of Statistics* (Vol. 1, Distribution Theory), 5th ed., Wiley, Chichester 1994.
- O. Tenaillon, J. E. Barrick, N. Ribeck, D. E. Deatherage, J. L. Blanchard, A. Dasgupta, G. C. Wu, S. Wielgoss, S. Cruveiller, C. Medigue, D. Schneider, and R. E. Lenski, Tempo and mode of genome evolution in a 50,000-generation experiment, *Nature* **536** (2016), 165–170.
- L. Wahl and A.D. Zhu, Survival probability of beneficial mutations in bacterial batch culture. *Genetics* **200** (2015), 309–320.

M.J. Wiser, N. Ribeck, and R.E. Lenski, Long-term dynamics of adaptation in asexual populations, *Science* **342** (2013), 1364–1367.

[dataset] M.J. Wiser, N. Ribeck, and R.E. Lenski, Data from: Long-term dynamics of adaptation in asexual populations, Dryad Digital Repository (2013), <https://doi.org/10.5061/dryad.0hc2m>.

A. Wünsche, D.M. Dinh, R.S. Satterwhite, C.D. Arenas, D.M. Stoebe, and T.F. Cooper, Diminishing-returns epistasis decreases adaptability along an evolutionary trajectory, *Nature Ecol. Evol.* **1** (2017), 0061.